ISTANBUL TECHNICAL UNIVERSITY ★ GRADUATE SCHOOL OF SCIENCE ENGINEERING AND TECHNOLOGY

PREPARATION AND CHARACTERIZATION OF ANTI BACTERIAL, ANTI SCRATCH AND EASY TO CLEAN MULTIFUNCTIONAL COATINGS BY SOL GEL METHOD

M.Sc. THESIS

Beyza Yedikardeş

Department of Nano Science and Nano Engineering

Nano Science and Nano Engineering Programme

JUNE 2016

ISTANBUL TECHNICAL UNIVERSITY ★ GRADUATE SCHOOL OF SCIENCE
ENGINEERING AND TECHNOLOGY

PREPARATION AND CHARACTERIZATION OF ANTI BACTERIAL, ANTI
SCRATCH AND EASY TO CLEAN MULTIFUNCTIONAL COATINGS BY
SOL GEL METHOD

M.Sc. THESIS

Beyza YEDİKARDEŞ
513141003

Department of Nano Science and Nano Engineering

Nano Science and Nano Engineering Programme

Thesis Advisor: Prof. Dr. Esra Özkan ZAYİM

Co-Advisor: Dr. Refika BUDAKOĞLU

JUNE 2016

İSTANBUL TEKNİK ÜNİVERSİTESİ ★ FEN BİLİMLERİ ENSTİTÜSÜ

ANTİ BAKTERİYEL, ÇİZİLME DİRENCİ YÜKSEK VE KOLAY TEMİZLENEBİLEN KAPLAMALARIN SOL JEL YÖNTEMİYLE HAZIRLANMASI VE KARAKTERİZASYONU

YÜKSEK LİSANS TEZİ

Beyza Yedikardeş
(513141003)

Nano Bilim ve Nano Mühendislik Anabilim Dalı

Nano Bilim ve Nano Mühendislik Programı

HAZİRAN 2016

Beyza Yedikardeş,, a **M.Sc.** student of ITU **Graduate School of Science Engineering and Technology** student ID **513141003**, successfully defended the **thesis** entitled "**PREPARATION AND CHARACTERIZATION OF ANTI BACTERIAL, ANTI SCRATCH AND EASY TO CLEAN MULTIFUNCTIONAL COATINGS BY SOL GEL METHOD**", which he prepared after fulfilling the requirements specified in the associated legislations, before the jury whose signatures are below.

Thesis Advisor :	**Prof. Dr. Esra Ozkan ZAYIM** Istanbul Technical University	....
Co-advisor :	**Dr. Refika BUDAKOĞLU** Şişecam Company, Science and Technology Center	....
Jury Members :	**Prof. Dr. Esra Ozkan ZAYIM** Istanbul Technical University	....
	Dr. Refika BUDAKOĞLU Şişecam Company, Science and Technology Center	
	Yrd. Doç. Dr. Mehmet Şeref Sönmez İstanbul Technical University	………………..
	Doç. Dr. Baki Altuncevahir İstanbul Technical University	………………..
	Yrd. Doç. Dr. Saffet Yıldırım İstanbul University	………………..

Date of Submission : 2 May 2016
Date of Defense : 10 June 2016

To my family and dearest friends,

FOREWORD

I would like to express my gratitude to my director of studies, Prof.Dr.Esra Özkan Zayim, whose expertise, understanding and patience, helped my work in this thesis.

I gratefully acknowledge Dr.Refika Budakoğlu for her endless patience, guidance and contribution in each part of this study. She always helped me to improve my knowledge in the area.

I would like to express my sincere acknowledgements to Şişecam Company, Science and Technology Center for giving me the opportunity to use their laboratories and materials. I had great lab periods with their support. Also I would like to thank to all my colleagues. It was a great opportunity for me to work with them and I will always remember the valuable times we had.

This thesis couldn't have been finished without the support of my friends. Their presence and care helped me overcome setbacks and stay focused on my graduate study. Especially, I would like to thank to Ezgi Deniz Biçer for her endless help.

Finally, I am deeply grateful to my father Özer Yedikardeş, my mother Elvan Yedikardeş and my sister Ceren Yedikardeş for their encouragement, trust and love.

June 2016   Beyza YEDİKARDEŞ
                                                                                      (Chemist)

x

TABLE OF CONTENTS

SYMBOLS

γ_{SL}	:interfacial tension between solid-liquid
γ_{SV}	:interfacial tension between solid-vapour
γ_{LV}:	:interfacial tension between liquid-vapour
$\emptyset_y$	:contact angle
H_s	:scratch hardness
P	:normal load
W	:width
H_0	:thickness
u_0	:withdrawal speed
μ, η	:viscosity
ρ	:solution density
σ	:surface tension
d	:depth of the scratch
R	.radius
$T\%$	:percent transmittance
I_0	:incident radiation
A	:absorbance
F	:shear stress
S	:shear rate
T	:torque
R_c	:inner diameter of cylinder
R_b	:diameter of spindle
ω	:angular rate
L	:length of spindle
n	:frequency
Tvis	:transmission in visible region
Tsol	:transmission in solar region
L^*	:lightness of the color
a^*	:position between magenta and green direction
b^*	:position between yellow and blue
S_N2	:nucleophilic substition reaction
KeV	:kilo electron volt
Pa	:pascal
GPa	:giga pascal
N	:newton
Cp	:centipoise
RPM	:revolution per minute
min	:minute
m	:meter
cm	:centimeter
mm	:milimeter
μm	:micro meter
nm	:nanometer
mL	:mililiter
gr	:gram

ABBREVIATIONS

CA	: Contact angle
ROS	: Reactive Oxygen Species
DNA	: Deoxyribo Nucleic Acid
ATP	: Adenosine Triphosphate
GLYMO	: (3-glycidyloxypropil) trimethoxysilane
TEOS	: TetraEthylOrtoSilicate
TMOS	: TetraMethylOrtoSilicate
EtOH	: Ethanol
E.Coli	: Eschericia Coli bacterium
S. **Aureus**	: Staphylococcus Aureus bacterium

LIST OF TABLES

LIST OF FIGURES

PREPARATION AND CHARACTERIZATION OF ANTI BACTERIAL, ANTI SCRATCH AND EASY TO CLEAN MULTIFUNCTIONAL COATINGS BY SOL GEL METHOD

SUMMARY

Developments of science and technology help us to understand the relationship between microstructure and material properties. Materials gain new properties by decreasing their particle size from micro to nano scale. Nowadays, thin film coatings on solid surface are developing by various physical and chemical coating methods. In order to show functionality, thin coatings must have homogeneous thickness and composition throughout the coating layer. Coating methods are generally divided as physical and chemical coating methods.

Among the coating methods, sol-gel method come forward as a chemical method to develop multifunctional coatings. In general, sol gel is defined as the transition from a liquid **sol** phase to solid **gel** phase. Sol-gel process does not require high process temperatures and in this process, there is a control of the material from precursor to final product at molecular level. It is a low cost process, capable to coat flat or geometric shapes and large areas as well. In addition, it allows us to produce organic-inorganic hybrid polymers, thanks to its high purity and homogenity. In hybrid compositions, organic polymers bring well adhesion and flexibility whereas inorganic molecules brings hardness. With these compositions, various functions such as thermal and chemical stability, antibacterial property, hardness, anti scratch, anti wear, wettability... etc, can be reached. In addition, hybrid coatings can easily be bonded to ceramic or glass surfaces, thanks to their covalent binding property.

Organofunctional silanes are the most suitable precursors for the preparation of organic - inorganic sol gel films. Alkyl groups which contain a functional groups such as epoxy, amino or vinyl are employed as cross linking agents in polymerization reactions. Meanwhile, non reactive groups of precursors do not participate polymerization reactions and they form porous structure in the silica network. This porous structure controls optical and mechanical properties of the films such as fracture or cracking. Since, the final product may have various characteristics depending on chemical composition of precursors, hydrolysis time, the addition order of materials into solution,etc..,sol-gel method requires close monitoring of each step.

In this study, various compositions containing (3-glycydyloxypropyl)trimethoxysilane (GLYMO), Titanium(IV)isopropoxide and $AgNO_3$ were prepared by sol-gel process. It is well known from the literature, coatings having Ag^+ on the surface present antibacterial properties. An experimental design of 27 different compositions were prepared by changing the amount of titanium(IV)isopropoxide, hydrolysing water and hydrolysis time. Glass substrates were coated by sol-gel dip coating method at 15 cm/min withdrawal rate. Wet coatings were cured in oven at 150°C for 30 min. For all set of coating compositions, physical tests such as, pencil hardness test, linear abrasion test,

adhesion test and nanoindentation tests were employed to find the most scratch resistant coating. The effect of the amount of last hydrolysing water on gel formation was investigated by percent solid test. From the exprerimental design set, it is found that, as the amount of Titanium(IV)isopropoxide decreases, the transparency and scratch resistance of the coatings decreased as well. For all the samples, a trend of decrease in solid % according to the increase in the amount of last hydrolysing water was obtained. Coatings which have high transparency were selected. Hydrolysis and polymerisation reactions of coating solutions and thin films were investigated by FTIR and silver absorbance during redox reactions were followed by UV absorbance spectroscopy. Micro and nano structural characterization of coatings were analyzed by SEM-EDS and AFM. Viscosity measurements in specific periods were done to determine the shelf life of the coating solutions. As a result of physical tests, the hardest and the most transparent samples were chosen to improve their easy to clean property. Fluorosilane was added to the most scratch resistant coating composition in two different route and easy to clean property of the coatings was determined by contact angle measurements. The anti bacterial activity of the coatings against Gram negative Eschericia Coli (E.Coli) and Gram positive Staphylococcus Aureus (S.aureus) was examined. Consequently, antibacterial (log5), scratch resistant (8N), and easy to clean (CA = 98-108°) multi-functional sol-gel coatings were developed.

ÇİZİLME DİRENCİ YÜKSEK, KOLAY TEMİZLENEBİLEN ANTİ BAKTERİYEL KAPLAMALARIN SOL JEL YÖNTEMİYLE HAZIRLANMASI VE KARAKTERİZASYONU

ÖZET

Bilimin ve teknolojinin gelişmesi, mikro yapı ve malzemenin özelliği arasındaki ilişkinin daha iyi anlaşılabilmesine imkân sağlamıştır. Malzemenin mikro yapısını oluşturan tanecikler nano boyuta indikçe malzemeler yeni özellikler kazanır. Günümüzde, önemli bir yer tutan katı yüzey üzerine ince film kaplamalar, çeşitli fiziksel ve kimyasal metotlarla elde edilebilir. İnce filmlerin istenen özellikleri gösterebilmeleri için uygun kalınlık, kompozisyon ve karakteristik özelliklere sahip olmaları gerekir.

Kaplama metodları arasında, sol-jel metodu çok fonksiyonel filmlerin eldesinde kullanılmasından dolayı öne çıkmaktadır. En genel haliyle, sıvı bir **sol** fazından, katı bir **jel** fazına geçiş olarak tanımlanır. Sol-jel metodu, yüksek proses sıcaklıkları gerektirmemesi, ön başlatıcıdan son ürüne kadar moleküler seviyede kontrolün sağlanması, diğer kaplama tekniklerine göre ekonomik olması ve düz yüzeylerin yanında şekilli yüzeylerin de kolay kaplanabilmesi sebebiyle hem organik ve inorganik, hem de organik-inorganik hibrit polimerlerin üretilmesine olanak sağlar. Hibrit yapılarda organik kısım yüzey yapışma ve esneklik özelliği kazandırırken, inorganik kısım ise çizilmeye ve aşınmaya karşı direnç sağlamaktadır. Sol-jel kaplamalar uygulandığı yüzeye kovalent bağlanma özelliği sayesinde, seramik ve cam gibi yüzeylere kuvvetli tutunurlar.

Organik-inorganik sol-jel kaplamaların hazırlanmasında en uygun çıkış maddeleri organofonksiyonel silanlardır. En az bir karbon-silikon bağı içeren silan bileşikleri, organosilan olarak adlandırılır. Organofonksiyonel silanlarda, silisyum atomuna karbon bağıyla bağlı olan ve reaktif olmayan alkil grupları ile yüksek reaktifliğe sahip alkoksi grupları vardır. Karbon-silikon bağı düşük yüzey enerjisine sahip, apolar ve oldukça kararlıdır. Alkil grupları, içerdikleri epoksi, amino, vinil gibi gruplar sayesinde polimerizasyon reaksiyonlarında çapraz ağ oluşturucu olarak görev yaparlar. Alkoksi grupları ise birbirleri ve ortamdaki su ile hidroliz ve kondenzasyon reaksiyonlarına girerler. Başlangıç malzemelerinin kimyasal kompozisyonu, hidroliz süresi, malzemelerin çözeltiye eklenme sırası gibi birçok parametre değiştirilebildiği için birbirinden çok farklı karakteristiğe sahip son ürünler elde edilir. Bu da, sol-jel yönteminin her adımının iyi analiz edilmesini zorunlu kılar. Sol-jel kaplamalar, uygulandıkların yüzeylere mukavemet, hafiflik, yüksek sıcaklığa ve aleve karşı direnç, UV ışığını kesme, parmak izi bırakmama, yüzeyde su tutmama, kolay temizlenebilirlik, korozyon direnci, aşınma ve çizilme direnci, anti mikrobiyellik gibi çeşitli özellikler kazandırılır.

Mikroorganizmalar cam ev eşyaları, endüstriyel sistemler, gıda paketleri, medikal malzemeler gibi çok çeşitli yüzeylere tutunabilirler. Mikrobiyel hücrelerin elektrostatik kuvvetler ve fiziksel etkileşimlerle geri dönüşümsüz olarak yüzey ile

bağlantı kurması ve bu yüzeyde çoğalması sonucu oluşan yapıya biyofilm denir. Su ile temas eden hemen hemen tüm yüzeylerde biyofilm oluşumu gözlenir. Bu yüzden mikroorganizmaların yüzeye tutunmasını, tutunduğu yüzeyde çoğalmasını ve biofilm oluşturmasını önlemek amacıyla antibakteriyel kaplamalar geliştirilmiştir. Yüzeyin topografisi ya da yüzey kimyası değiştirilerek, polimerizasyon yöntemiyle antimikrobiyel ajanların polimer matrikse tutunması sağlanır. Antibakteriyel yüzeylerin etkinliğini artırmak için hidrofobik özellik gösterebilen, uzun zincire sahip, pozitif yüklü moleküller tercih edilir. Katı yüzeylerin ıslanabilirliği endüstride kullanılan önemli bir özelliktir. Malzemenin yüzey pürüzlülüğü değiştirilerek hirdofobik yüzeyler süper hidrofobik yüzeylere dönüştürülebilir. Doğadaki lotus çiçeğinden esinlenilerek oluşturulan bu yüzeyler, su damlasının kir partiküllerini toplayarak kendi kendine kaymasını sağlar, böylece kirlenen yüzeyin temizliğini kolaylaştırır. Ancak, hidrofobik sistemler çizildiklerinde v-eya aşındıklarında, doğal sistemler gibi kendilerini yenileyemezler. Bu yüzden yüzey koruyucu kaplamalara ihtiyaç duyulur. Aşınmaya ve çizilmeye karşı direnci yüksek olmayan malzemeler, sol-jel tekniğiyle kaplanarak dayanıklı hale getirilir. Hibrit organik-inorganik silika sistemlerde kullanılan organofonksiyonel silanlar, polimerizasyon reaksiyonları sırasında çapraz ağ oluşturucu ajan olarak görev yaparlar. Uygulandıkları yüzeylere kovalent bağlarla bağlanarak kaplamanın yüzeye güçlü bir şekilde tutunmasını sağlayarak, malzemenin mekanik özelliğini artırırlar.

Tez çalışmasında, sol-jel prosesiyle çizilme direnci yüksek, kolay temizlenebilen antibakteriyel kaplamaların geliştirilmesi hedeflenmiştir. Kaplama çözeltisi (3-glisidoksipropil) trimetoksisilan (GLYMO), Titanyum (IV) isopropoksit ve Gümüş Nitrat ve etanol içermektedir. GLYMO, kaplamalara esneklik ve içerdiği epoksi grupları nedeniyle mukavemet/yüzey tutunma özellikleri vermesi, Titanyum (IV) isopropoksit ise sertlik ve ağyapıcı olması amacıyla kullanılmıştır. Gümüş Nitrat, su ve birçok çözücüde kolaylıkla çözünerek kaplama sistemine girmesi nedeniyle ilave edilmiştir. Çizilme direnci yüksek antibakteriyel kaplamaların elde edilmesi amacıyla bir deneysel tasarım planı oluşturulmuştur. Kaplama prosesinde üç etkin değişken (ön hidroliz süresi, Titanyum (IV) isopropoksit miktarı, son hidroliz için eklenen su miktarı) seçilmiş ve her bir değişken içerisinde 3 seviye (süre, gramaj) belirlenerek (n^3) 27 farklı kaplama kompozisyonu içeren bir deney seti tasarlanmıştır. Cam altlıklar, daldırarak kaplama tekniğiyle 15 cm/dk çekiş hızında tek kat kaplanarak, 150°C'de 30 dk sürede kürlenmiştir. Elde edilen kaplamaların öncelikle kalem sertlik testi, lineer aşınma, yapışma testi, geçirgenlik ve nano indentasyon testleri yapılmıştır. Deneysel tasarım planı çerçevesinde elde edilen kaplamalar incelendiğinde, ilave edilen Titanium(IV)isopropoksit miktarı azaldığı zaman kaplamaların geçirgenliği ciddi anlamda düştüğü ortaya çıkmıştır. Jelleştirilen kaplama çözeltilerinin % katı hesabı yapılmış ve tüm örnekler birarada değerlendirildiğinde, son hidroliz için ilave edilen su miktarı artırıldıkça % katı değerleri düştüğü ortaya çıkmıştır. Bu sonuç, hidroksil ve alkoksil yer değişiminden kaynaklanmaktadır. Saydamlığı ve çizilme direnci yüksek olduğu belirlenen kaplamaların çözelti hallerinde hem FTIR ile hidroliz ve polimerizasyon reaksiyonları incelenmiş ön hidroliz süresinin en etkili değişken olduğu belirlenmiştir. Ayrıca, hazırlanan kaplama çözeltilerinin raf/kullanım ömürlerinin belirlenmesi amacıyla çözeltilerin belirli periyodlarla viskoziteleri ölçülmüştür. Kaplama içerisine eklenen Gümüş Nitratın, kaplama hazırlık prosesi içerisinde belli aşamalarda UV absorbansları ölçülmüş ve hidroliz esnasında gümüş iyonun absorbansının arttığını, son hidroliz ile birlikte gümüş iyonunun absorbansının

tamamen yok olduğu tespit edilmiştir. Dolayısıyla, gümüş iyonunun (Ag^+), kaplama matrisinde yer alan hidroksil grupları ile tepkimeye girerek gümüşe (Ag^o), indirgenip ağ içerisine yerleştiği varsayılmıştır. Aynı aşamalarıda yapılan pH ölçümlerinde de pH değerlerinin ilk hidrolizle 4.6'dan 4.3'e ve son hidrolizle birlikte pH=3'e inerek daha asidik bir çözelti haline gelmesi de kaplama çözeltisindeki gümüşün indirgenerek hidroniyum (H^+) iyonlarını ortaya çıkardığını desteklemektedir. Kaplamaların yüzeyden elemental kimyasal analizi ve kaplama kalınlığı SEM-EDS ile, yüzey morfolojisi ise AFM analizleriyle değerlendirilmiştir. Özellikle, AFM analizinde, kaplama yüzey morfolojisinde nanoboyutta gümüş zenginleşmesi gözlenmiştir.

Karakterizasyon ve fiziksel testler sonucunda seçilen kaplama örnekleri antibakteriyel aktivite testlerine maruz bırakılmıştır. En yüksek çizilme direnci veren kaplama kompozisyonuna florosilan ilavesiyle kolay temizlenebilirlik özelliği sağlanmıştır. Kolay temizlenebilirlik, temas açısı (CA) ölçümleriyle belirlenmiştir. Anti bakteriyel, çizilme direnci yüksek ve kolay temizlenebilen kaplamaların, Gram negatif Escherichia Coli (E.Coli) ve gram pozitif Staphylococcus Aureus (S.aureus) bakterilerine karşı anti bakteriyel aktivite testi yapılmış ve log 5 = %99.999 seviyesinde yüksek antibakteriyel özellik tespit edilmiştir. Sonuç olarak, çizilme direnci yüksek (8N) ve kolay temizlenebilen (CA=98-108°) antibakteriyel (log5) kaplamalar geliştirilmiştir.

1. INTRODUCTION

In recent years, nanocrystalline silver has attracted attention because of its physical and chemical properties that differ from macro crystalline silver. Although there are various inorganic antibacterial materials that have been studied for many years, among these inorganic nanoparticles, silver has been considered as one of the most efficient antibacterial agent. Antibacterial surfaces are developed by different methods. In all methods that are used for getting antibacterial surfaces, contact killing plays an important role. Silver nanoparticles can interact with the cell membrane of bacteria. Many researches have shown that silver ions are able to damage cell membranes and lead to inactivation of DNA replication.

With the growing public health awareness, usage of antibacterial coatings has increased in many application areas such as biomedical, implants or food packaging. Recent advances in materials science and nanotechnology methodologies present various available options to design surfaces in addition to anti bacterial property. However, the usage of biodegradable and edible thin films has been limited because of some problems such as mechanical performance, fabrication and cost [77]. In order to obtain multifunctional coatings, hybrid systems are employed. Hybrid systems are systems, which have characteristics of both inorganic and organic materials. This combination of organic and inorganic properties within the same material creates new possibilities in terms of mechanical, electrical or optical properties. They contribute to the increase of scratch resistance, durability, easy to clean property and flexibility of the coatings.

Surface protective coatings, which provide protection against corrosion, wear and scratch are vital applications of glass materials. The mechanical behaviour such as hardness, elastic modulus and toughness are responsible for the coating resistance. Scratch deformation of polymeric surfaces has become an important area of research in materials science and mechanics. Commercially available colloidal silica nanoparticles are mostly preferred to improve mechanical, chemical and physical

properties due to their fine particle size distribution and high surface area. They increase cross linking density in the system thanks to high number of hydroxyl groups.

Easy to clean coatings are widely used for commercial applications. There are two possible routes to produce easy to clean surfaces. One method is to make the surface hydrophilic by way of using either TiO_2 or some tensides to wash away any dirt or powder. The other method is to make the surface hydrophobic by using fluorosilanes or other branched alkyl silanes. Hydrophobic property is related to wettability of the surface. Since the surface energy between water and air is less than water and solid, surfaces tend to reduce surface energy. It creates a liquid solid contact area. Hydrophobic surfaces prevent polar molecules to be adsorbed by the surface interface. Dirt particles stick on the surface and water droplets clean the surface bringing dirt with them due to gravity [78]. In this study, silane coupling agent Fluorosilane was used to give easy to clean propety to the coating. Branched silanes are silicon based chemicals that can react with inorganic substrates to form covalent bonds such as glass. So, they are water repellent, easy to clean and very useful for sol gel systems.

The aim of this study is to produce antibacterial thin films, which have anti scratch and easy to clean functions as well. In this study, 3-Glycidoxypropyltrimethoxysilane is used together with Titanium (IV) isopropoxide to form a hybrid coating system that has strong adhesion with glass surface. 3-Glycidoxypropyltrimethoxysilane is one of the most popular functionalized silane which is modified with epoxy group [73]. It is primarily used as a chemical intermediate and as adhesion promoter in coatings. 3-Glycidoxypropyltrimethoxysilane used in many applications such as protective antiscratch coatings [74], anticorrosion layers [75] and optical limiting devices [76]. Due to its epoxy group, it can strongly bind covalently to the surface. Epoxy groups act as coupling agents that make crosslinkings in the polymerization reactions. The formation of the network is due to hydrolysis and condensation reactions. After opening the epoxy ring, different reactions may be observed. Final structure and opening the epoxide ring depend on the pH, temperature and solvent composition [79, 80, 81]. Titanium (IV) isopropoxide has higher reactivity than silicon alcoxides. It allows us to have better completion of hydrolysis-condensation

2

reactions and high degree of cross linking. Therefore, in this thesis study, it was aimed to develop a coating that is flexible and hard by using GLYMO and Titanium (IV) isopropoxide.

The sol gel chemistry provides a very useful way to produce desired mixtures that control the hydrolysis and condensation reactions. It allows us to control and unify all the steps at the molecular level. The process does not require vacuum environment or high temperatures. The biggest advantage of sol gel technique is to provide multifunctionality to the coatings. In this study, sol gel method was used to produce anti bacterial, anti scratch and easy to clean thin films.

1.1 Functional Surfaces

Because of the high surface area to volume ratio, surface properties of nanoparticles can significantly affect the interfacial energy and intermolecular forces between particle and polymer surface. In recent years, several functional coatings have been worked and modified with additional functions such as hydrophobic, anti bacterial, anti scratch or photocatalytic [44]. Incorporation of nanoparticles into polymer matrix represents new kind of properties. As a result, the material may exhibit advanced mechanical, thermal or optical properties. But the key point is aggregation of nanoparticles. There are basically two ways to overcome this problem; modification to surface with small sized inorganic nanoparticles or grafting polymeric molecules that can covalently bind to the particles. There is a significant demand for particularly anti bacterial coatings, which is able to prevent material surface for production of microorganisms. Therefore, polymeric nanocomposites have attracted significant attention.

Hydrophobic surfaces are very useful mainly because of less cleaning demand. But, they can not heal themselves like natural systems when they are damaged or scratched. Therefore, there is a need for mechanically enhanced coatings.

1.1.1 Antibacterial mechanism

Among the inorganic nanoparticles, silver has been considered as the most effective antibacterial agent. Silver nanoparticles show new properties when compared to bulk state of silver, due to its mechanical, chemical and optical properties [45]. Many

factors can influence the antimicrobial effect of materials; for instance size, shape, charge, surface coating, dose..etc [46]. In this study silver nanoparticles have been used as antibacterial agent in the form of silver nitrate. Silver salts have been used medically in controlling of bacteria and other organisms. The release of incorporated of antibacterial agent is achieved by diffusion into the aquous medium, degradation or hydrolysis of covalent bonds. [47] The bacterial adhesion depends on the attraction between cell and the surface. The factors including bacterial adhesion on the surface are Van der Waals forces, Brownian motion, gravitational forces, hydrophobic interactions, electrostatic forces, surface roughness, topography and physical configuration [88], [89].

There are basicly two approaches for designing antibacterial coatings, however the mechanism is not fully understood.

1. Bacteria Repelling

A reason of permanent contamination is bacteria that attach to surface and form biofilms. Bacteria in biofilms, such as antibacterial glass coatings, are more responsive to biocides. Since, it is very difficult to remove biofilm on the surface, preventing bacterial adhesion has been used as a key point [48]. Anti adhesive surfaces does not include any toxic compound and does not damage the bacterial flora.[49] Bacterial adhesion at biomaterial surfaces is often described as a two stage model. At stage one, adhesion occurs through a combination of non-specific physicochemical interactions. At the stage two, a specific binding of cell surface proteins to biomolecules adsorbed by the abiotic substrate [50]. Subsequently, the usage of physical surface modifictions enable us to prevent bacterial adhesion on the surface.

2. Contact Killing

In spite of the fact that the antibacterial mechanism of silver is not fully explicable, typically four mechanism are suggested at the present time; direct attack and damage to cell membrane, generation of reactive oxygene strains, disruption of ATP production and interruption of DNA replication [51]. It's believed that silver ions inhibit dehydrogenation processes and lead to an increase in reactive oxygen species (ROS) associated with DNA damage [52]. When silver ion react with water, it is

oxidized. Oxidizing silver releases free radicals. These free radicals may lead to produce hydrogenperoxide. Hydrogen peroxide is very toxic in bacteria cell. On the other hand, free radicals are higly reactive with other substances because of having unpaired electrons. These unpaired electrons make atoms unstable. In order to reach stable state, they steal an electron from other surrounding substances. This causes several destructive chain reactions in bacteria cell. Therefore, they kill the bacteria rupturing cell memrane and dividing DNA into the small pieces. In some cases, it is accepted that heavy metals react with –SH groups of proteins for deactivation [53]. Thiol groups are very important groups of proteins responsible for enzymatic activity. Heavy metals react with proteins by combining the thiol groups and cause the inactivation of proteins. Furthermore, silver can cause deposition of proteins in vitro. Therefore, entrance of silver into bacteria may lead to protein deposition in baceria cells. Subsequently, DNA turns into a condensed form. All these phenomenas lead to the damage or death of bacteria cells.
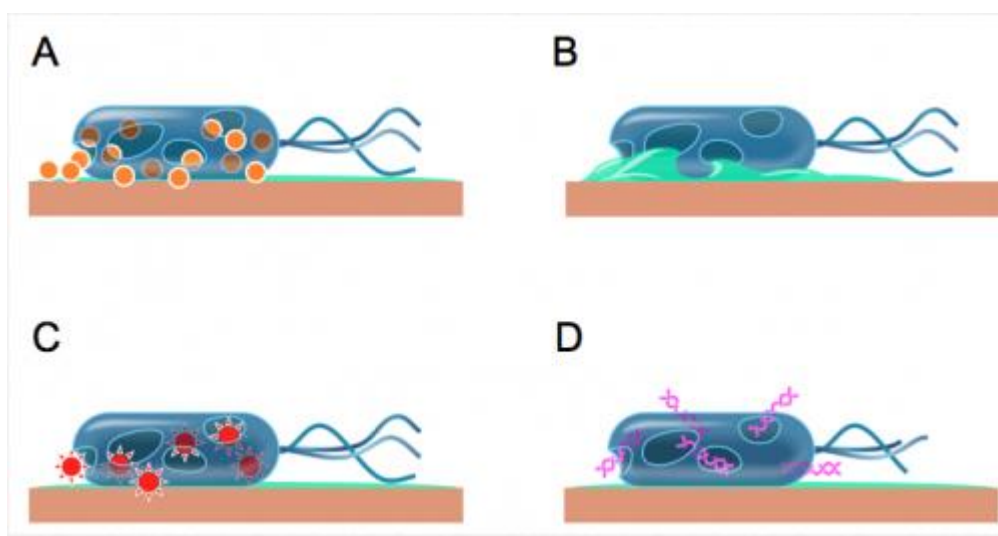
Figure 1. 1 : Contact killing mechanism (A) Attacking to the cell membrane (B) Rupturing cell membrane (C) Leading to the generation of toxic radicals (D) Destruction of DNA

1.1.2 Hydrophobicity

Inspired by the Lotus flower in nature, humans have started to mimic surface of Lotus leaf to design self-cleaning surfaces. Measuring wettability of materials is evaluated by measuring the contact angle. The contact angle, ϑ, is the angle between liquid – solid interface. When a solid is wetted by a liquid, there are three possible;

solid- liquid, solid- air and liquid- air. The relation between interfaces and contact angle has been described by Young Equation (1.1) by Thomas Young. [55]

$$\gamma_{lv}.\cos\emptyset_Y = \gamma_{sv} - \gamma_{sl}$$

(1.1)

where γ_{lv}, γ_{sv} and γ_{sl} is liquid-vapor, solid-vapor and solid-liquid and $\emptyset_Y$ is contact angle, respectively.
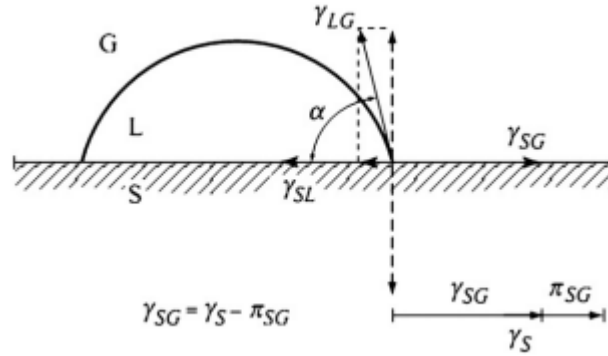
Figure 1. 2 : Relation between interfacial tensions and contact angle.

It is considered that, there are three types of chemical bonds to be able to explain better surface energy and contact angle; covalent, ionic and metallic bonds. These intermolecular forces to interract with surface is defined as surface tension. It is responsible for the shape of water droplet. In general, high contact angles between liquid and solid lead to high adhesive forces. For low contact angles ($\vartheta < 90°$), the droplet spreads over and wets to the surface and it is called hydrophilic. Hydrophilic molecules have high Hydrogen bonding and they are mostly polar. For high contact angles ($\vartheta > 90°$) droplet does not spread over the surface and it is called as hydrophobic. Since wettability is poor, contact angles minimizes. Hydrophobic surfaces in water attract each other, the total energy of the system reduces by minimizing the area exposed to water. For a hydrophobic surface, energy is required to wet the increased surface area created by the rough surfaces whereas decreasing contact angle created by the smooth surfaces. There is also one more surface called as superhydrophobic which the contact angle of a water droplet is higher than 150°. For superhydrophobic surfaces, there is almost no contact with the surface. [54]

6
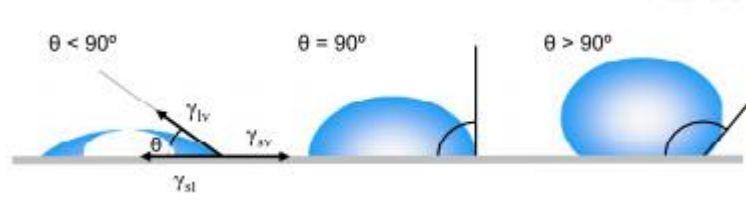
Figure 1. 3 : Illustration of water droplets

1.1.3 Scratch resistance (Anti scratch)

In general, to improve mechanical properties of a polymeric system, silica nanoparticles, silicate layers, core shell particles or metal oxides are introduced to the system. The desired property often changes depending on providing good dispersion of the nanoparticles in the polymer matrix. Particle dispersion controlled by surface modification to prevent agglomeration. Because, aggregation of the nanoparticles can lead to reduce of mechanical properties [72]. There are strong interactions between particle cores that can cause to aggregation if the surface are not functionalized. Therefore, the core-shell nanoparticle structure forms by using encapsulation in order to enhance menhanical property.

Many researchers have reported [82] an increase in scratch resistance of coating with increasing colloidal silica content. Through the low cost and usefulness for matrix adhesion, aquous colloidal silica has been used to improve coating properties such as hardness, anti-scratch, anti-blocking and so on.

Scratch hardness H_s is determined as;

$$H_s = \frac{8P}{\pi w^2}$$

(1.2)

Where P is the normal load and w is width of the scratch [85]. Considering only plastic deformation, w can be calculated as;

$$W = 2\sqrt{2Rd - d^2}$$

(1.3)

Where d is depth of the scratch and R is Radius of indenter.

7

The mechanical behavior of coatings containing silane was recently investigated using nanoindentation, nano scratch and micro-hardness tests. [83]

In addition, nano-rainforced coatings have become popular in recent years owing to their improved mechanical properties and heat stability. Rainforcement materials are materials which are able to affect composite properties such as strength, toughness or thermal stability. Rainforced nanomaterials give the material distinctive properties [87]. Reinforced materials are used as filler by adding into a polymer matrix. A filler material provides more siffness to the polymer matrix. Not only mechanical properties, but also optical and electrical properties are improved by this method.

1.2 Thin Film Deposition

Thin films are the layer materials which, their thicknesses changes from nanometre to micrometre scale. Technology of applying a very thin film of material is called as thin film deposition. Technology of thin films enable us to control deposition process and physical properties of a material.Thin film deposition can be applied onto a substrate to be coated or onto a previously coated layer. In our day, there are several deposition techniques to produce thin film, but mainly they are divided into two categories; physical techniques and chemical techniques. Since, sol-gel method used in this study, only sol gel processes will be explained among deposition techniques.
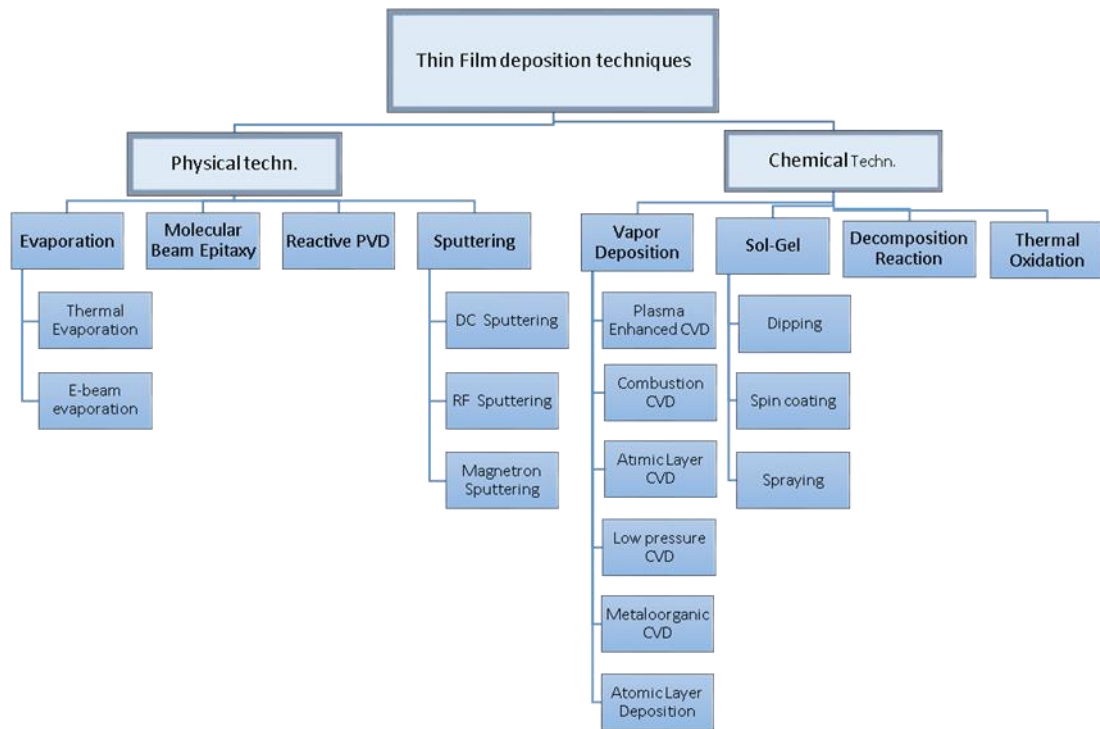
Figure 1. 4 : Classification of thin film production techniques.

1.2.1 Sol-gel route

The earliest sol gel derived materials have been reported by Ebelman in 1845 at the Manufacture de Sevres in France [1]. He prepared the first alkoxide from $SiCl_4$ and alcohol [2]. When the chemicals exposure to the atmosphere, they formed a gel. This is the first form of the sol-gel process as known today. Hamilton and MacKenzie [3], Luth and Ingamells [4], Hamilton and Handerson [5], and Bigger and O'Hara [6] all described distinct variations of same process. Although the term sol gel has been used in 1939's, the number of scientific researches have gradually increased after the article of Dislich [7]. Sol-gel coating systems were widely studied at Schott Glass in early 1950's [8]. The initial works have been appeared on the preparation of mainly TiO_2 and SiO_2. Because of increasing interest of many investigators in the sol-gel process, multicomponent glass systems and silicate materials are developed. For last

decade, strength-building studies are sustained by means of sol gel technique in order to produce more lightweight glass materials.

The sol gel process is a process by which a solution undergoes a transition state to form a three dimentional network of polymer chains. Main material dissolves in a solvent by a series of hydrolysis and polimerization reactions and turns out a sol. In general, sol is defined as a liquid with colloidal particles, which are not dissolved. The colloid particles that have a diameter of 1-100 nm [67]. Wan der Vaals and electrostatic forces between substrate and coating are stronger than gravitational force, materials of sol do not form a precipitate. If these molecules expanded in sol, they reach a bigger structure and compose a gel. Through this process, homogeneous inorganic oxide materials with attractive properties of hardness, optical transparency, chemical strength, altered porosity, and thermal resistance, can be produced at room temperatures [9].
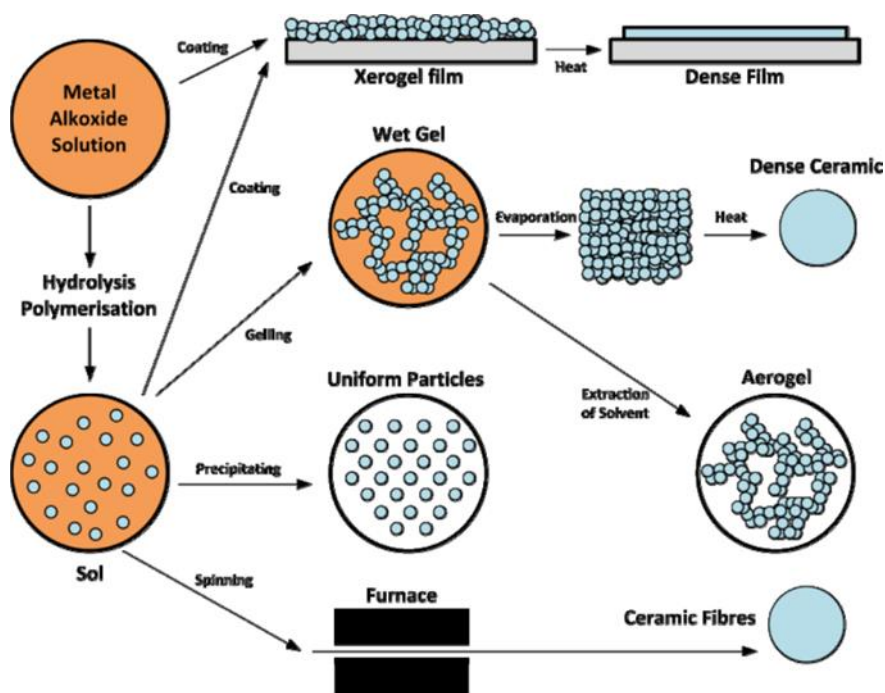
Figure 1. 5 : Sol-gel steps and final products.

The method involves simply basic steps [10] which are described below.

10

Hydrolysis

Hyrdolysis is initiated by the addition of water to the organic solution, which involves Silane under acidic, neutral or basic conditions. Acids and bases have different reaction mechanisms to catalyze hydrolysis and condensation. At the functional group level, three main reactions are used to describe in the sol-gel process; hydrolysis, water condensation and alcohol condensation. In general, hydrolysis is performed by S_N2 type reaction [11]. For an alkoxy silane system, the water initiates formation of reactive Si-OH groups. S_N2 mechanism generally include three following steps. First step is nucleophilic addition of OH⁻ ion to Si atom. It increases the coordination number of positively charged metal atom and leads to formation of transition state. In the second step, positively charged metal atom is transferred to alkoxyl group and consequently protonated R-OH ligand removed. Central atom always have high hydrophilic strength. If acid is added at the first step as catalyst, reactive cationic species are formed. This step is rate-determining step and causes to S_N1 type mechanism. The acid catalyzed mechanism involves slow hydrolysis, whereas the base catalyzed mechanism involves rapid hydrolysis. Slow hydrolysis results in weakly cross linked systems. [12]
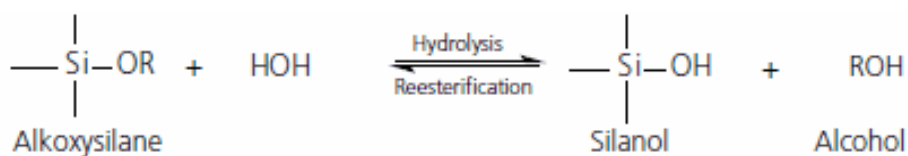
Figure 1. 6 : Hydrolysis reaction

.
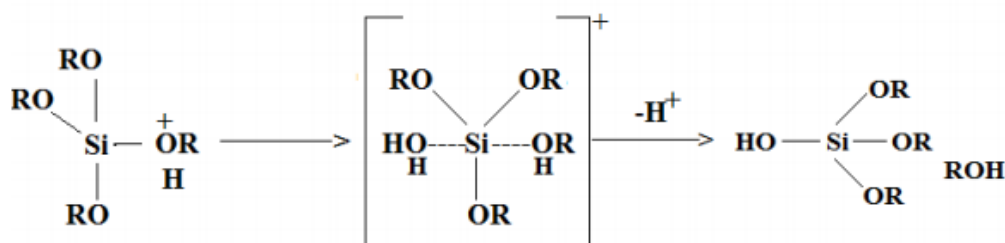
Figure 1. 7 : Acid catalysed hydrolysis reaction.

Gelation (Polycondensation)

A gel is an interface system which has high amount of liquid between solid and liquid phase. Gelation is related to shape of colloidal particles. Gel molecules bind each other with strong or weak forces. Therefore, they fill the vacancies and form a framework. Gels are microelastic materials which have micron sized pores.

Gelation process is based on hydrolysis and polycondensation reactions. In the condensation step, silanol groups reacts to form Si-O-Si bridges. The capability of bridging bonds increase during the condensation. Increasing amount of silanols, hydroxyl groups are lost and more cross-linking occurs to form a three dimentional network. Depending on the acid addition, dissolution of silica particles become negligible, surface is protonated and condensation rate is increased. [69]
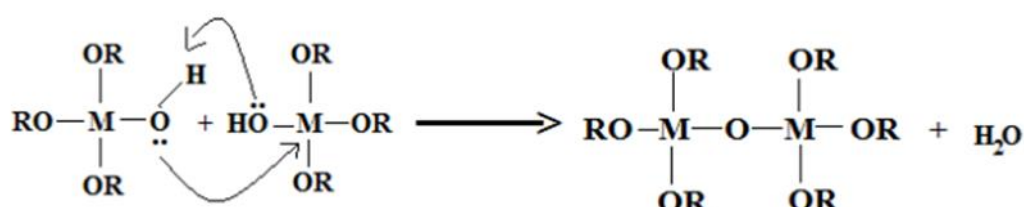
Figure 1. 8 : Acid catalysed condensation reaction.

Polymeric oxide gels are obtained from metal alkoxides. When the water adds, metal alkoxide hydrolyzed. Polymers in the sol gets bigger by means of condensation reaction. After for a while, a big polymer mass spreads to the entire solution. This point is the point of transition from solution to gel and called as gelation point. Polymeric oxide network structure forms by controlling rate of hydrolysis and condensation reactions.[66] Different rates of hydrolysis and polycondensation reactions cause to different polymeric structures at the gel point.
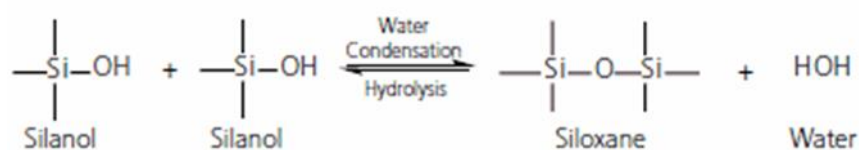
Figure 1. 9 : Water condensation reaction.

Gels are sometimes defined as strong or weak depending on the bond strength. Polymerization to form siloxane bonds occurs by either an alcohol producing condensation reaction or water producing reaction [15]. Usual partial charge calculations on the transition state, alcohol producing condensation is kinetically preferred. [16]
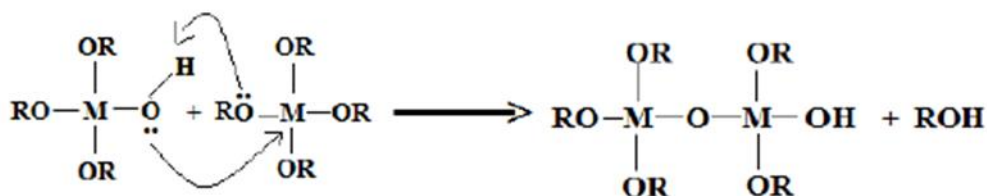
Figure 1. 10 : Acid catalysed alcohol producing condensation.

Condensation reaction is slower than hydrolysis. In the final step of gelation, water and organic solvent vaporize from vacancies of glass. Volume of solid matrix increasingly shrinks. During the drying step, some smaller pores soaked with solvent whereas some bigger pores are empty. Consequently, a dry gel which is termed xerogel forms [13]. Xerogels are mechanical stable, transparent and immiscible in many organic solvents and water [14].

Aging

Aging is the step which is following the hydrolysis and condensation reactions. The structure and properties of material changes during aging time. Diverse types of phase transformations can occur during aging. For instance, a liquid can be separated into two or more phases [17]. Aging also may lead to crystallization. The stiffness and strength of gel increase with aging [18], so aged gels shrinked and crack less. The structure of the gel, temperature, pH and time affect aging process interfacial energy and phase transformations [19],[68]. Increasing aging periods, porousity of gel also increases.

Drying

Drying process can be explained as removing surplus of the sol. The process of drying a porous material can be divided into several steps. At first, body schrinks by

an equal amount of liquid volume. Liquid-solid interface remains out of the body. When the body becomes too stiff to shrink, second step starts. Liquid leaves air-filled pores near the surface. When the air captures pores, liquid film continuously flux to the exterior. Therefore, vaporization continues to occur from surface of the body. [9]

In order to remove silanols on the surface, stabilization is required. Therefore, it prevents re-hydrolysis and structural changes. The last step of drying is densification. In this step, gel is converted into glass. Some bonds are broken and new ones form. In general, this step occurs simultaneously.

Figure 1. 11 : Reaction scheme of sol-gel route.

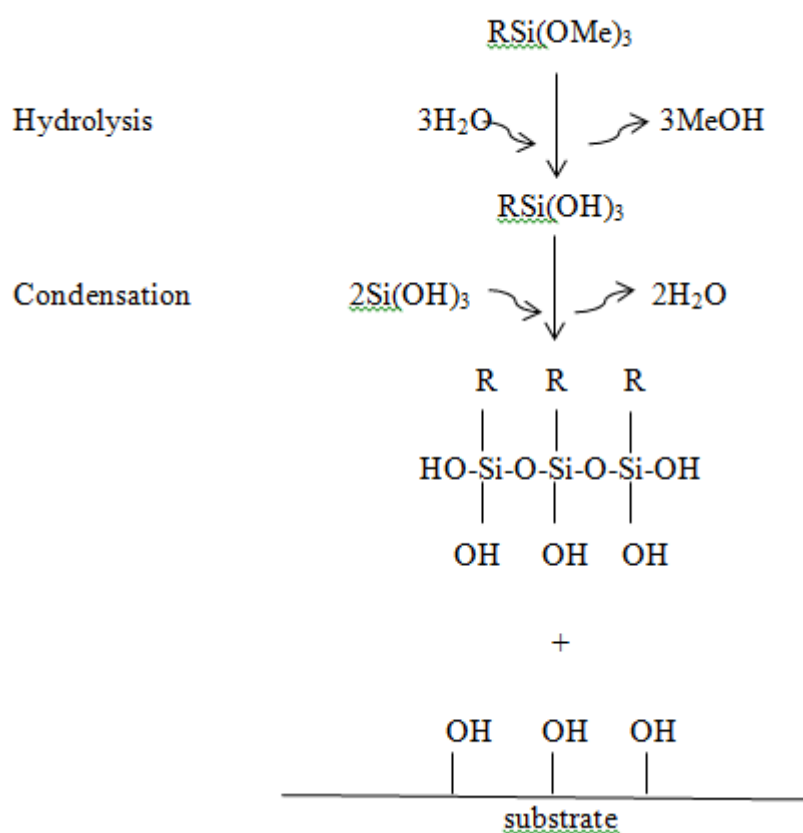During drying or curing, covalent bond occurs with the substrate with loss of water. These reactions occur fast and simultaneously after the hydrolysis step.

1.2.2 Components of sol-gel

1. Precursors

All the soluble precursors can be used in sol-gel process. They can be categorised inot two main titles; metal salts and alkoxides. [20]

Metal alkoxides have the following general formula, $M(OR)_x$ where M is metal, R is an alkyl group and x is also valence number of metal. These materials are considered as the best starting materials to prepare sol-gel components [21]. Transition metals (Ti,Zn) are generally used molecular precursors for glass and ceramic materials. Because of their high electrophilicy, they become low electronegative. Therefore, they are less stable for hydrolysis, condensation and some other nucleophilic reactions. The most common alkoxides are tetraalkoxysilane and tetrametoxysilane which are abbreviated as TEOS and TMOS [22]. Since metal alkoxides contain reactive OR group, they can enter to reaction effectively. Physical properties of metal alkoxides can be varied by changing alkyl group or soluble metal ion. Most of alkoxides are volatile and can be purify by means of distillation. Many of the alkoxides are very difficult to be obtained since they are very sensitive to atmospheric moisture. Subsequently, oxide mixtured must be obtained by adding water to medium.

2. Solvent

Solution chemistry of metal salts and metal alkoxides are quite different.Thus, solvent is selected depend on the type of precursors. The solvents are classified as non-polar, polar aprotic, and polar protic solvents. If solvents can exchange a proton, it is named as protic and it is named as aprotic when they can not do. Types and amount of solvents in sol mixture directly affect hydrolysis kinetic, particle size, physical properties and transparency of gels. [23]

3. Catalyst

In general, hydrolysis and condensation are take place simultaneously, so it is difficult to predict kinetic behavior. In acidic solutions, condensation reactions are slower than hydrolysis. Although mineral acids or ammonia are most generally used

in sol-gel processing, other known catalysts are acetic acid, potassium hydroxide, amines, potassium flourine, hydrogen florine, titanium alkoxides, and vanadium alkoxides and oxides [24]. In the acid-catalyzed reaction, the first step is the protonation of an alkoxyl group. Positive charge develops on the alkoxysilane through the attack of an acid catalyst. The positive charged of the protonated alkoxide is correspondingly reduced, making alcohol a better leaving group. As the alcohol leaves, -OH group loses a proton and becomes positively charged. If the steric crowding around the silicon atom reduces, hydrolysis rate increases. This mechanism leads to reaction limited cluster aggregation supporting the condensation reaction between clusters and silicon atom. Reaction limited cluster aggregation occurs both under acidic and basic conditions [25].

1.2.3.Techniques of sol-gel method

There are several coating techniques using with sol gel method. These techniques has classified below; a) Dip Coating, b) Spin Coating,c) Spray Coating,d) Laminar flow,e) Imprint sol-gel,f) Roll coating, etc.

Since dip coating technique enables to create different film thicknesses and provides high homogenitiy, dip coating technique was used in this study.

Dip coating

Among the available techniques, dip coating is the most widely used for deposition applications. It is well enough simple. It has low cost and high coating quality [26]. Dip coating is the process by which enable us to deposit of a wet liquid film by using a liquid coating medium. The coating process may be divided to four steps; immersion, deposition, drainage and evaporation. At first, substrate is immersed in a liquid to be coated. After several seconds, substrate is withdrawn from coating tank with a constant rate. It requires a mechanical system by which is able to move with a constant rate [27]. The deposition operations are automated by a computer controlling system. It allows to different thickness can be achieved. The relationship between the withdrawal speed and thickness of the thin film has been examined by Landau and Levich [70].

$$h_0 = 0.944 \frac{(\mu u_0)^{2/3}}{\sigma^{1/6}(\rho g)^{1/2}} = 0.994 \, (Ca)^{1/6} \left(\frac{\mu u_0}{\rho g}\right)^{1/2}$$

(1.4)

Film thickness is controlled by rate of withdrawal, coating viscosity and content of solution. [30] Increasing speed, film thickness also increases.

After coating, liquid is drain from the surface. Consequently, the solvent evaporates from the fluid and dried by heating. At the evaporation step, sol particles form a transparent film [28]. Film formed is condensed by heat treatment. After coating process, samples are heated up to 100°C - 180°C. Heat temperature is determined by solution composition. [29]

The final film structure depends on some parameters such as the structure of inorganic species in the sol, reactivity of these species, evaporation rate and so on.

immersion   withdrawal   consolidation   curing
                               drying   sintering
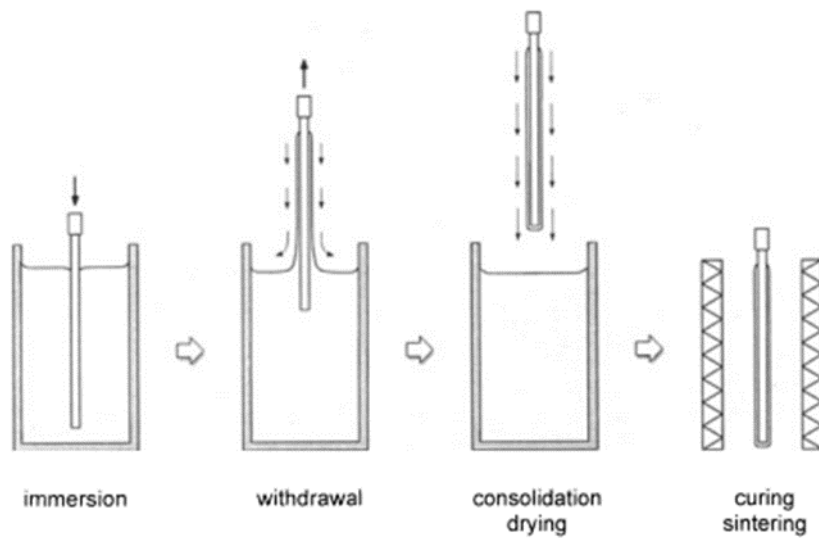
Figure 1. 12 : Fundamental stages of sol gel dip coating.

1.2.4 Advantages and disadvantages of sol-gel process

Advantages

- Production of new organic-inorganic hybrid materials which do not exist naturally. [31]

- High degre of uniformity, obtaining very pure products.

17

- Excellent chemical homogenity in the final product.

- Minimizing chemical interactions between the material and solution tank walls.

- Easy to control kinetics of various chemical reactions.

- Easy to control particle shape and size. It allows to control growth of colloidal particles.

- Ability to use multi-layer coatings.

- It uses low processing temperatures except condensation step. [32]

- A simple, effective and economic method.

- Can mixed different precursors. Thus, it allows homogenius and controlled doping.

- Can control aging and drying conditions. Therefore, mechanical strength and particle size can be controlled.

- Can create very fine powders.

- New nanocrystalline solids outside the range of normal glass.

Disadvantages

- High cost of the initial ingredients.

- More complicated and time consuming.

- Large schrinkage during processing.

- Residual hydroxyls, residual carboxyls.

- Health hazards of organic solutions.

1.2.5 Applications of sol-gel process

Sol-gel process has been used historically in order to produce materials in various size, shape and configuration. In the last century, it was used for glasses [33], ceramics [34], biomedicals [35], chemical sensors [36], fibers [37], membranes [38], optical sensors [39], photochromic applications [40] and electronics. Moreover, it was widely used for optoelectronics [41], electrochromics, ferroelectrics [42], solar cells [43] and high-strenght coatings as a coating method.

2. TESTS AND CHARACTERIZATION

2.1 Tests

2.1.1 Pencil hardness test

A mechanical hardness test pencil (Erichsen Pencil Hardness Test Model 318) consist of a spring loaded Tungsten carbide. The hardness is defined as the minimum load or force on the ball point. If the spring pressure is too high, scratchs are visible with naked eye. If the pressure is low, no scratch appears. The applied spring pressures can change in three range; blue marked spring is used for 0 – 3N, red marked spring is used for   0 - 10 N and yellow marked springs is also used for 0 - 20N ranges. The tip of the pencil produce scratch on the surface by moving the pencil back and forth motion.

2.1.2 Adhesion test

Adhesion test (Elcometer 1542 Cross Hatch Adhesion Tester) is a test provides adhesion analysis by seperating coating from substrate. A lattice pattern scratches the film using a cross hatch cutter. Test area brushes to remove any film particles. A special tape applied over the crossed are and detached quickly by pulling the tape back off. This test depends to the American Standard Test Method (ASTM) conditions. Therefore, appearance of the area is compared with ASTM standards.
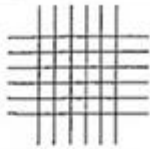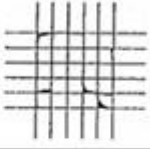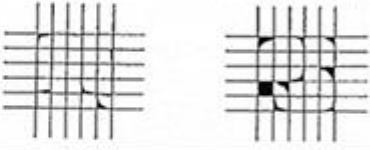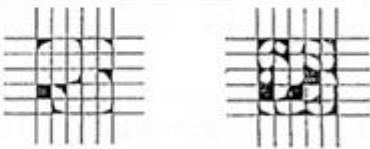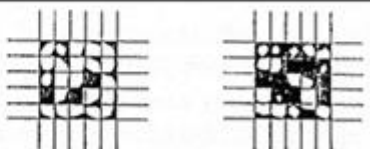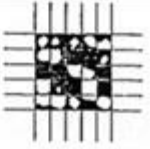
Classification	% of Area Removed	Surface of Cross-cut Area From Which Flaking has Occured for 6 Parrallel Cuts & Adhesion range by %
5B	0% None	
4B	Less than 5%	
3B	5 - 15%	
2B	15 - 35%	
1B	35 - 65%	
0B	Greater than 65%	

Figure 2. 1 : Adhesion test ASTM standards.

2.1.3 Nanoscratch test

First mechanical properties of sol- gel thin films have been studied by Fabes by using microindentation [71]. For all that, elastic modulus and hardness mesurements have been demonstrated. Two contact techniques were used to employed; nanoindentation and nanoscratch. Nanoscratch test can be used for characterizing adhesion failure of thin films and coatings. Scratch resistance is determined by deformation and delamination mechanism using frictional force and imagining scratches after test. Sharp indenter tip is applied onto the surface, and moves smultaneously in a lateral direction [86]. For the scratch test, we used cone diamond tips with a tip radius of 5

μm and the 90° tip inclination. Nanoscratch values of coatings were measured by Nanovea M1 Scratch Tester.

2.1.4 Linear abrasion

Abrasion resistance is one of the most studied measurement technique of liquid repellent surface durability. This test allows to remove a portion of the surface by means of mechanical treatment. [62] The instrument consist of an arm, a laser alignment guide and a setting table. It is programmable to 1000 cycle. The arm with a felt moves back and forth on an object periodically such as coated glass material and creates an erosion. After abrasion test, an alteration in contact angle, transmission and mass of the sample can be measured . In this study, Taber Industries Linear Abraser Model 5750 was used. The test was held constant at 60 cycles/min speed and the measurements were taken each 500 cycles.

2.1.5 Antibacterial activity test

Antibacterial activity is that difference in the logarithm of the viable cell on the anti-bacterial treated product and untreated product after inoculation and incubation of bacteria. The determination of the antibacterial activity (microbicidy) of surfaces is described in the following norms: ISO 22196 and JIS Z 2801. These norms are reliable and quick. ISO 22196 is used against both E.Coli (gram negative) and S.Aureus (gram positive) organisms. 50mm x 50mm specimens were prepared for treated and untreated samples. Throughout the analysis, optimum temperature was kept at 37°C for production and growth of bacteria. Colony forming unit (CFU/ml) and reproduction rate of selected bacteria species were studied. After sterilization of selected samples, 100 μl inoculum which consists 10^4 CFU/ml was planted and waited for 1 hour at 37°C. Therefore, it was provided samples to touch inoculums. Then, samples were removed from solid medium and incubated for 12 h. at 37°C. At the and of the 12 hours, the number of viable bacteria is calculated and compared before incubation. The percent reduce of bacteria activity is calculated with formula below;

% reduction = ((A-B)x100) / A   (2.1)

A: microorganism number before incubation

B: microorganism number after incubation

Log reduction $= \log_{10}(A/B)$ (2.2)

1 log reduction : 90% reduction

2 log reduction : 99% reduction

3 log reduction : 99,9% reduction

4 log reduction : 99,99% reduction

5 log reduction :99,999% reduction

2.2 Characterization

2.2.1 Scanning electron microscopy (SEM)

Scanning electron microscopy enables us to investigate specimens with a resolution down to the nanometer scale with an electron beam.Pictures on the microscope are formed by secondary electrons and back-scattered electrons.A basic SEM instrument (Jeol JSM-6010LV) involves a light source,an illumination section,a magnification section and a detector.

The basic principle is that a beam of electrons is generated by an electron gun and accelerated to an energy in the range 0,1-30 keV. A series of lenses control the diameter of the beam to focus the beam of the specimen. Beam passes through the apertures which is holes in metal film and reach beam/specimen area. Several types of signals generate an interaction. The signal is acquired by detector. Consequently, it is converted to an image or spectra on the monitor display. All of these interactions occur at vacuum level.When the beam focuse on the specimen surface, magnification or specimen area is changed.[56]
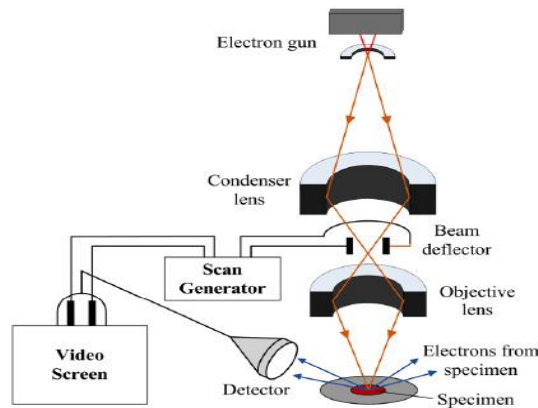
Figure 2. 2 : SEM system operation diagram.

2.2.2 Energy dispersive spectroscopy (EDS)

EDS (connected to SEM with Oxford software) is an analytical instrument which allows to identify chemical and elemental analysis of a sample. At first, an X-Ray spectrum generated from the scanning area of SEM by means of inelastic collusions of electron beams. EDS involves a semiconductor detector. A very small current is produced from the semi-conductor [56]. The EDS detector converts the energy of X-ray's into a voltage. When an incident X-ray comes to the detector, energy is absorbed by electron-hole pairs. As soon as the electron is raised into the conduction band, it leaves behind a hole. This hole behaves like positive charge in the crystal. A higher energy shell fills the hole and creates an energy difference. The energy of the X-rays emitted by specimen. This energy allows the elemental composition of the specimen to be measured. [57]

2.2.3 Atomic force microscopy (AFM)

Atomic Force Microscopy (Veeco Digital Instrument, NanoScope) allows us to see a shape of a surface in 3D details on nanoscale by measuring forces bertween a sharp probe. The basic imaging prinicple is simple. A sharp tip of a cantilever is brought onto the sample attached to a piezocrystal. Therefore, it provides to control in three dimension [58]. A laser is focused onto the tip of the cantilever and the detector captures the reflected film. Images are formed by interaction forces between tip and surface. [59]
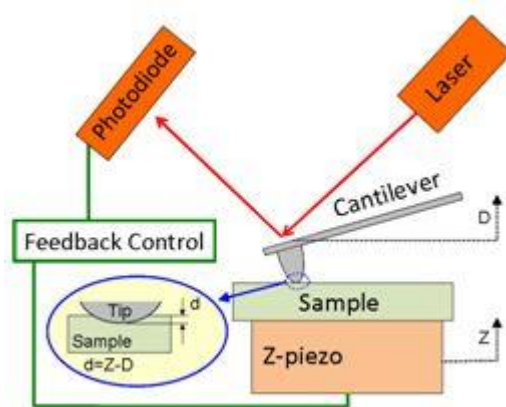
Figure 2. 3 : AFM system operation.

2.2.4 Fourier transform infra red (FTIR)

Absorbtion in IR region induces vibrational and rotational status of the molecules. The absorbtion frequancy depends on the vibrational frequency of the molecules. IR spectroscopy gives information about functional groups of molecules and measures vibrational frequency of variable bonds in the molecule.a molecule absorbs infrared light only if it has a dipol moment. [60]

The basic principle of fourier transformation is the same with IR spectrometry but the only difference is that FTIR (Bruker Vertex 70 Platinum) enable us to do measurement by applying mathematical method. Compared to dispersive IR analysis,FTIR is faster and gives better signal-noise ratio. [61]

2.2.5 Contact angle measurement

In this work, we measured contact angles by static sessile drop method. This method is realized by an optical sub-system to capture the profile of a liquid on a solid substrate. The angle between the liquid/solid interface and the liquid/vapor interface is the contact angle. In this study, KSV Instruments CAM200 contact angle meter was used in order to measure contact angles with high resolution cameras. The instrument includes four micro liter syringes. 5 mL water was dropped onto the coated surfaces from syringe. 5 images were taken for each second of droplet during totally 5 seconds. Ultimate contact angle were obtained taking the average on left and right side contact angles of water droplet.

2.2.6 UV-VIS spectroscopy

A UV spectrophotometer uses light over the ultraviolet range (185 – 380 nm) and visible range (380-700 nm). It consist of a light source, prism or holographic gratings, detector and optic lens. A prism or grating generate light spectra into many colors foe analysing. Detector converts light signal into electrical signal. Optic lenses focuse light through the instrument. Mainly there are two types of UV spectrophotometer. In a single beam spectrophotometer, the light beam directly passes through the sample. In the double beam spectrophotometer, light source is split into two separate beams and then it pass through the sample. When the light beam passes through the sample, the amount of light absorbed is calculated as the ratio between incident radiation (I_0) and transmitted radiation. [90] Transmittance is defined as;

$$\%T = \frac{I}{I_0} \times 100$$

(3.1)

The relationship between absorbance and % transmittance is defined as ;

A=2 - log(%T)   (3.2)

2.2.7 Transmission measurement

A Hazemeter (BYK Gardner GmbH, Transmission Haze) indicates transmission haze of films and other materials. The instument can measure transmittance, haze and clarity in a simple way. The working principle is that a light source comes throught the sample, and the system measure the light scattered for transparent or translucent materials. Haze is defined as percentage of scattered light. Transmission is defined as the percentage of transmitted to incident light. Transmission and haze are used for interpreting transparency of a sample.

2.2.8 pH measurement of the coating solution

After the calibration pf pH meter, electrodes are dipped into solution. Pressed the measure button. After the pH icon stops flashing, recorded pH value of the sample are measured.

2.2.9 Viscosity of the coating solution

Viscosity is defined as a liquid's resistance to flow. When a liquid flows, one portion of the liquid moves with respect to neighboring portions. Cohesive forces within the liquid create an internal friction which reduces the rate of flow. Intermolecular forces are weak in low viscosity liquids such as ethanol or water. Increasing intermolecular forces, viscosity of a liquid increases. On the other hand, viscosity can be explained by hydrogen bondings. Having stronger intermolecular forces cause to flow more slowly. [63], [65]. Viscosity is defined mathematically by this simple formula;

$$\eta = Viscosity = \frac{F}{S} = \frac{Shear\ stress}{Shear\ rate}$$

(3.3)

$$\mu = \frac{T(R_c - R_b)}{4\pi^2 R_b^3 nL}$$

(3.4)
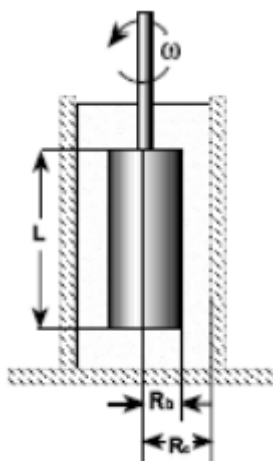
Figure 2. 4 : Image of cylinder spindle.

The fundamental unit of viscosity measurement is the centipose (cP) whereas SI unit of viscosity is Pascal (10 P = N.s.m^{-2}). During this study, viscosity of solutions are measured by Brookfield DV-I Prime Viscosimeter by using UL adapter, cylinder spindle and temperature controller. To make a viscosity measurement, 16 ml solution was taken and put into UL adapter. Desired speed setting is selected. Spindle was immmsersed into tank. After that, tank and spindle assembled to water jacket and viscosimeter. Water jacket was connected to temperature controller and set the temperature 25°C. The instrument measures torque and then converts to a viscosity as centipoise and displays automatically on the screen. The spindle multiplier constant is used to calculate viscosity range at any spindle speed. For the UL adapter,

spindle multiplier code is 0.64, torque constant is 1 and shear rate constant is 1.223. Using these constants, shear rate and viscosity range are calculated as given below.

Viscosity Range [cP] = Torque const. x Spindle mult. cons. x 10000/RPM   (3.5)

Shear Rate [sn $^{-1}$] = Shear rate const. x RPM   (3.6)

If the torque is directly proportional with viscosity, these type of liquids are called as ''Newtonian Fluids''. If the viscosity is inversely proportional with liquid, it is called as ''Non-Newtonian Fluids''. [64] Ketchup, blood, yoghurt and mud can be given as Non-Newtonian fluids. Fluids like water and gasoline are Newtonian fluids.

2.2.10 Percent solid test

This test is used for determination of the non-volatile content of the solids in the sample. Non-volatile residue determined as a material which remains after evaporation under specific conditions. At first, a certain amount of solution is taken and measured with dish. Then, they dried in oven at 105°C 30 min. The difference in weight of the dish and solid, before and after drying, represent the volatiles. And the amount of solid remains is calculated as percent solid.

3. EXPERIMENTAL SECTION

3.1 Preparation of Glass Surfaces

Flat glass samples were used as substrates for the coatings. Glass samples were supplied from Trakya Cam Factory by Şişecam Science and Technology Center. Throughout the experimental study, 4 mm thickness and 5 cm x 5 cm size glass samples were used.

Ultrasonic cleaning is very precise and powerful to clean even the hardest impurities and contaminations effectively. Before starting the experiments, glasses were washed by WV120/90 FinnSonic Ultrasonic Cleaner. The instrument consists of 5 tanks. First tank contains KOH solution, second tank contains deionized water, third tank contains acidic H_3PO_4 solution and fourth and fifth tanks contain deionized water. Tanks were first heated to 60°C before soaking the glasses. Glass samples were inserted into a basket and immersed into the first tank (basic) for 9 min by selecting agitation and ultrasonic mode. After 9 min, they were rinsed in the second tank. After that, they immersed into the third tank (acidic) for 9 min. again and rinsed in the second tank again, then rinsed in fourth tank and fifth tank, respectively. Finally, glasses dried in CRD 90 FinnSonic drying oven for 10 min. at 100°C.
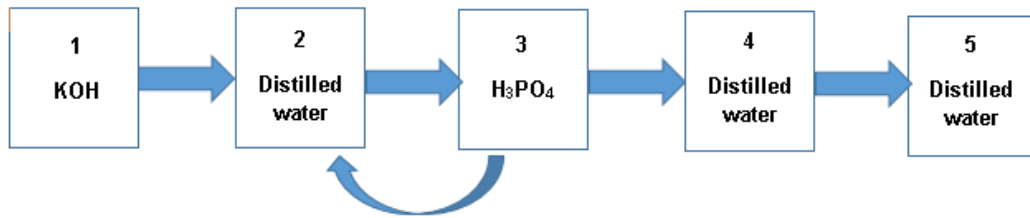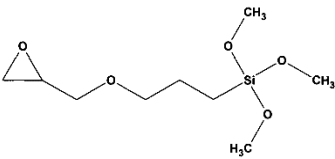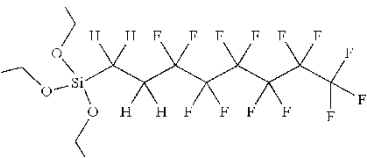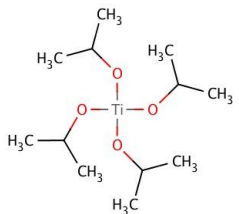

Figure 3. 1 : The scheme of cleaning process.

3.2 Preparation of Coating Solutions

The chemicals used throughout the thesis study are written below. They were used as received.

Table 3. 1 : Table of chemicals used in thesis study.

Chemical Name	Chemical Formula	Chemical Structure	Purity	Producer
3-Glycidyloxy propyltrimethoxy silane (GLYMO)	$(H_3CO)_3Si-(CH_2)_3-(OCH_2)-CH(O)CH_2$		>%98	Evonik
3,3,4,4,5,5,6,6,7,7,8,8,8-tridecafluorooctil triethoxysilane	$C_{14}H_{19}F_{12}O_2Si$		>%95	Evonik
Titanium(IV) isopropoxide	$Ti[OCH(CH_3)_2]_4$		>%95	Alfa Aesar
Silver Nitrate	$AgNO_3$		Extra pure	Merck
Ethanol	CH_3CH_2OH		>98	Merck

At start, a stock solution of silver as 3% (gr/gr) AgNO3/Ethanol was prepared by dissolving silver nitrate in absolute Ethanol. An experimental design of 3 parameters (pre-hydrolysis time, amount of Titanium(IV)isopropoxide, final hydrolysis water amount) and 3 levels of the parameters were determined. So, 27 (n3) experimental points were set to find the optimum sol-gel process condition to develop antiscratch and antibacterial coating (Table 3.1).

50 gr of GLYMO is mixed with 50 gr of silver stock solution in (1:1) ratio. Then, 4 gr of deionized water added drop by drop into the mixed solution and stirred on a magnetic stirrer at the room temperature for ½ /1 / 2 hours. After that, 10/30/40 gr of Titanium (IV) isopropoxide was directly added into total solution under stirring. After 5 min. later 30 gr % 3 Ag-EtOH solution and 5/10/20 gr distilled water were added and stirred until cooling at room temperature. Eventually, a clear yellow coloured solution was obtained.

Figure 3. 2 : The recipe of coating solution

Table 3. 2 : Experimental design of 3 levels of 3 parameters.

Name	Pre-hydrolysis time	Final amount of $Ti[OCH(CH_3)_2]_4$	Final amount of H_2O
Sample 1	½ h.	10 gr	5 gr
Sample 2	½ h.	10 gr	10 gr
Sample 3	½ h.	10 gr	20 gr
Sample 4	½ h.	30 gr	5 gr
Sample 5	½ h.	30 gr	10 gr
Sample 6	½ h.	30 gr	20 gr
Sample 7	½ h.	40 gr	5 gr
Sample 8	½ h.	40 gr	10 gr
Sample 9	½ h.	40 gr	20 gr
Sample 10	1 h.	10 gr	5 gr
Sample 11	1 h.	10 gr	10 gr
Sample 12	1 h.	10 gr	20 gr
Sample 13	1 h.	30 gr	5 gr
Sample 14	1 h.	30 gr	10 gr
Sample 15	1 h.	30 gr	20 gr
Sample 16	1 h.	40 gr	5 gr
Sample 17	1 h.	40 gr	10 gr
Sample 18	1 h.	40 gr	20 gr
Sample 19	2 h.	10 gr	5 gr
Sample 20	2 h.	10 gr	10 gr
Sample 21	2 h.	10 gr	20 gr
Sample 22	2 h.	30 gr	5 gr
Sample 23	2 h.	30 gr	10 gr
Sample 24	2 h.	30 gr	20 gr
Sample 25	2 h.	40 gr	5 gr
Sample 26	2 h.	40 gr	10 gr
Sample 27	2 h.	40 gr	20 gr

3.3 Coating Process

In this study, glasses were coated with coatings solutions by Dip-Coating technique. KSV Nima Dip Coater, Single Vessel Medium was used for dip coating. The instrument has maximum 1000 mm/min and minimum 50 mm/min withdrawal speed. During the coating process, glass substrates were dipped into the solution vertically. Immersion speed and waiting time in the solution were kept constant. Glasses were coated in clean room to exclude dust at 23°C. Before coating, each properly cleaned glass sample were exposed to air compressor to get rid of any dust attached on the surface. The template was dipped into the sol and withdrawn at 15 cm/min, left to dry in air in the vertical position for a couple of min. Coated glasses were placed into a pre-heated furnace. Carbolite PN 200 furnace was used in this study. The temperature and time of the curing process was set at 150°C for 30 min.

3.4 Gelation Process

In order to get gels for the SEM-EDS and FT-IR analysis, 5 mL of sol was weighted and put into the furnace at the same given temprature and given time.

Figure 3. 3 : Image of gelated solution after furnace.

3.4 pH Measurement of Coating Solution

At first, pH and temperature of GLYMO was measured as 4,61 at 22,8°C. After addition of 3% Ag-EtOH and water, pH decreased to 4,35 at the same temperature. Addition of Ti(IV)isopropoxide didn't change the pH value but the temperature of solution increased to 29,8°C. At the end of the 3% Ag-EtOH and water addition for last hydrolysis reduced pH to 3.

4. RESULTS AND DISCUSSION

4.1 Optimization of the Anti Scratch and Anti Bacterial Coating Composition

The aim of the experimental design was to determine the most transparent and scratch resistant antibacterial coatings. Although, all the samples have strong adhesion to the glass surface and sample no of 4,5,6,13,14,15,22,23,24 were the most scratch resistant coatings in their group according to the Pencil Hardness test. And, these samples were chosen for chemical, structural and morphological analysis. From the experimental design set, it is found that, as the amount of Titanium(IV)isopropoxide decreases, the transparency and scratch resistance of the coatings decreased as well.

Table 4. 1 : Physical measurement of test samples.

Name	%T (550 nm)	Adhesion	Pencil Hardness
Sample 1	82,9±0,67	5 B	2 N
Sample 2	81,3±0,69	5 B	2 N
Sample 3	81,0±0,63	5 B	1 N
Sample 4	90,3±0,00	5 B	7 N
Sample 5	90,3±0,00	5 B	7 N
Sample 6	90,3±0,00	5 B	8 N
Sample 7	89,9±0,06	5 B	5 N
Sample 8	89,9±0,08	5 B	5 N
Sample 9	86,4±0,94	5 B	5 N
Sample 10	81,5±0,30	5 B	4 N
Sample 11	81,5±0,30	5 B	4 N
Sample 12	82,1±0,26	5 B	5 N
Sample 13	89,7±0,10	5 B	5 N
Sample 14	90,0±0,10	5 B	6 N
Sample 15	90,0±0,10	5 B	6 N
Sample 16	89,0±0,20	5 B	2 N
Sample 17	89,5±0,10	5 B	2 N
Sample 18	89,7±0,07	5 B	5 N
Sample 19	80,9±0,10	5 B	1 N
Sample 20	81,8±0,15	5 B	1 N
Sample 21	82,3±0,10	5 B	1 N
Sample 22	90,1±0,00	5 B	7 N
Sample 23	90,2±0,06	5 B	8 N
Sample 24	90,2±0,06	5 B	8 N
Sample 25	90,0±0,10	5 B	1 N
Sample 26	90,0±0,10	5 B	1 N
Sample 27	90,0±0,07	5 B	1 N

4.2 Percent Solid Test

As can be seen from the table below, for all sets as the final amount of water addition increases the solid% decreased. This shows the exchange of alkoxide groups with OH groups leading to the polymerization. For all the samples, a trend of decrease in solid % according to the increase in the amount of last hydrolysing water was obtained.

Table 4. 2 : Percent solid amounts of test samples.

Before Oven			After Oven		
Sample Name	Dish (g)	Sol (g)	Dish+Sol (g)	Dish+Sol (g)	Vaporized (g)	Solid%
1	3,02	2,02	5,04	3,64	1,40	30,70
2	2,28	2,01	4,83	3,40	1,43	28,90
3	2,91	2,01	4,92	3,44	1,48	26,40
4	2,45	2,04	4,49	3,10	1,39	31,90
5	2,30	2,02	4,32	2,93	1,39	31,20
6	2,48	2,05	4,53	3,08	1,45	29,30
7	2,27	1,97	4,24	2,92	1,32	33,00
8	2,65	1,58	4,23	3,16	1,07	32,30
9	2,37	2,05	4,42	2,96	1,46	28,80
10	2,90	2,05	4,95	3,53	1,42	30,74
11	2,66	2,04	4,70	3,25	1,45	28,99
12	2,52	2,19	4,71	3,12	1,59	27,40
13	2,91	2,17	5,08	3,62	1,46	35,50
14	2,32	2,11	4,43	2,97	1,46	30,81
15	2,87	2,04	4,91	3,45	1,46	28,44
16	2,50	2,02	4,52	3,15	1,37	32,20
17	2,62	2,02	4,64	3,25	1,39	31,20
18	2,82	2,71	5,53	3,62	1,91	29,52
19	2,48	2,63	5,11	3,27	1,84	30,04
20	2,71	2,15	4,86	3,32	1,54	28,40
21	2,47	2,05	4,52	3,02	1,50	26,83
22	2,97	2,21	5,18	3,67	1,51	31,70
23	2,77	2,37	5,14	3,47	1,67	29,54
24	2,74	2,12	4,86	3,83	1,03	28,40
25	2,10	2,10	4,20	2,78	1,42	32,39
26	2,26	2,16	4,42	2,91	1,51	30,10
27	2,04	2,38	4,42	2,72	1,70	28,58

4.3 Linear Abrasion Test

According to the physical tests results, nine samples were choosen and compared to each other. Consequently, Sample 23 was determined as the most resistant to the test. And this solution was taken as a basic referance solution to be modified for hydrophobicity.

Table 4. 3 : Comparison of transmission values of test samples.

Name	%T before taber abrasion (with apparatus)	%T after taber abrasion (without apparatus)	%ΔT
Sample 1	31,7	29	-2,7
Sample 2	32,3	28,7	-3,6
Sample 3	32,9	29	-3,9
Sample 4	36,3	31,6	-4,7
Sample 5	36,1	31,7	-4,4
Sample 6	34,8	31,6	-3,2
Sample 7	35,4	34,9	-0,5
Sample 8	36,2	34,9	-1,3
Sample 9	35,6	34,9	-0,7
Sample 10	32,8	32,1	-0,7
Sample 11	31,8	29,9	-1,9
Sample 12	32,5	31,1	-1,4
Sample 13	34,8	36,5	-1,6
Sample 14	36,1	35,4	-0,4
Sample 15	34,6	36,5	-1,8
Sample 16	32,5	33,8	-1,4
Sample 17	34	33,8	-0,2
Sample 18	36	33,8	-2,2
Sample 19	31,6	30,9	-0,7
Sample 20	32,3	31,5	-0,8
Sample 21	32,4	31,8	-0,6
Sample 22	37,2	36	-1,2
Sample 23	36,2	36,1	-0,1
Sample 24	36,2	36,1	-0,1
Sample 25	35,2	35,9	0,7
Sample 26	35,7	36,3	0,6
Sample 27	36	36	0,4

4.4 Elemental Composition and Thickness Measurements of Samples by SEM-EDS

For all the chosen gel samples same amount % of each element were obtained. That is, 45% for O, 25% for Si (Table 4.4). Also, all the samples had approximately same thicknesses (Table 4.5). So, it can be said that from SEM-EDS analysis, there were not significant differences in chemical composition and thicknesses.

Table 4. 4 : Percent compositions of solution contents.

Sample	%O	%Si	%Ti	%Ag
4	45,41	27,72	19,92	6,94
5	45,21	27,33	20,25	7,21
6	44,97	26,88	20,64	7,50
13	44,58	25,01	23,29	7,13
14	45,16	26,86	21,03	6,96
15	44,66	25,23	23,04	7,07
22	44,97	26,46	21,40	7,18
23	44,89	26,14	21,82	7,15
24	45,02	26,41	21,50	7,00

Table 4. 5 : Average thickness of test samples.

Sample	Average thickness (µm)
4	1,56
5	1,20
6	1,12
13	1,57
14	1,21
15	1,21
22	1,25
23	1,40
24	1,31

4.5 FTIR Analysis of the Coating Solutions

First, FTIR of the precursor GLYMO which has the coupling function in coating sols were taken (fig. 4.1) and the characteristic peaks of GLYMO are analyzed (Table 4.6)
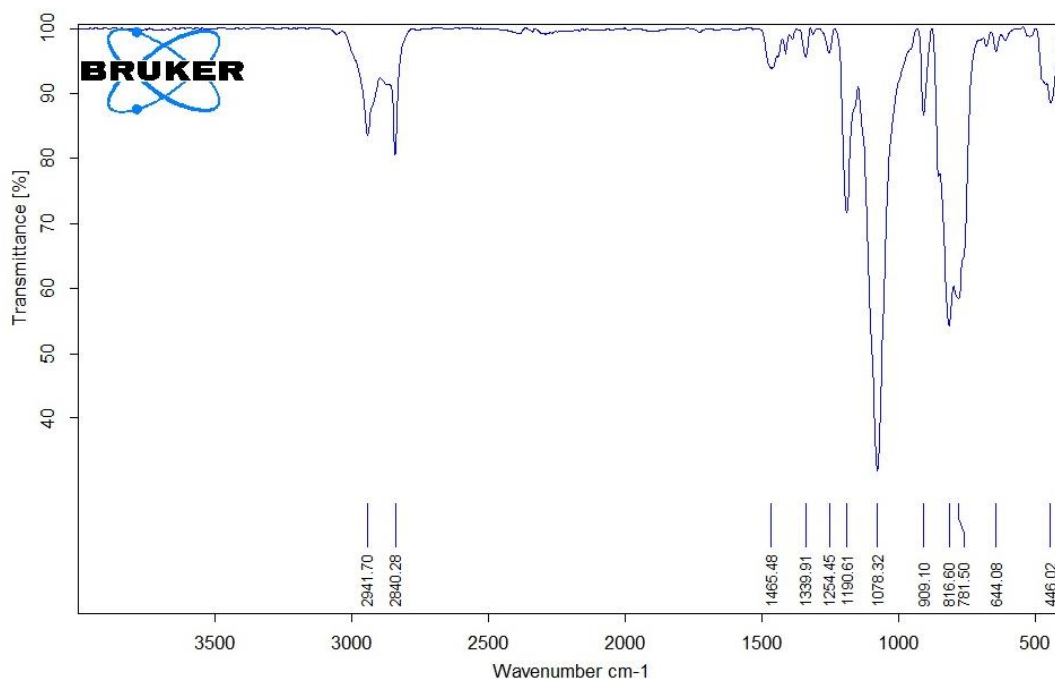
Figure 4. 1 : FTIR peaks of GLYMO starting material.

Table 4. 6 : Characteristic peaks of GLYMO starting material.

Wavenumber (cm-1)	Assignment
2941,284	C-H symmetric streching
1190	Methyl group in Si-O-CH3
1139,1254	C-O-C epoxy ring breathing
1078,816,718	Si-O-C streching
1465	CH2 deformation
909	C-O-C epoxy
1465	epoxy CH2 bending

Table 4. 7 : Changing parameters of 3 final samples.

Sample	Pre-hydrolysis time / min.	Ti (iOPr)$_4$ / gr	Amount of water / gr
S5(blue)	30 min.	30 gr	10 gr
S14 (red)	60 min.	30 gr	10 gr
S23(yellow)	120 min.	30 gr	10 gr
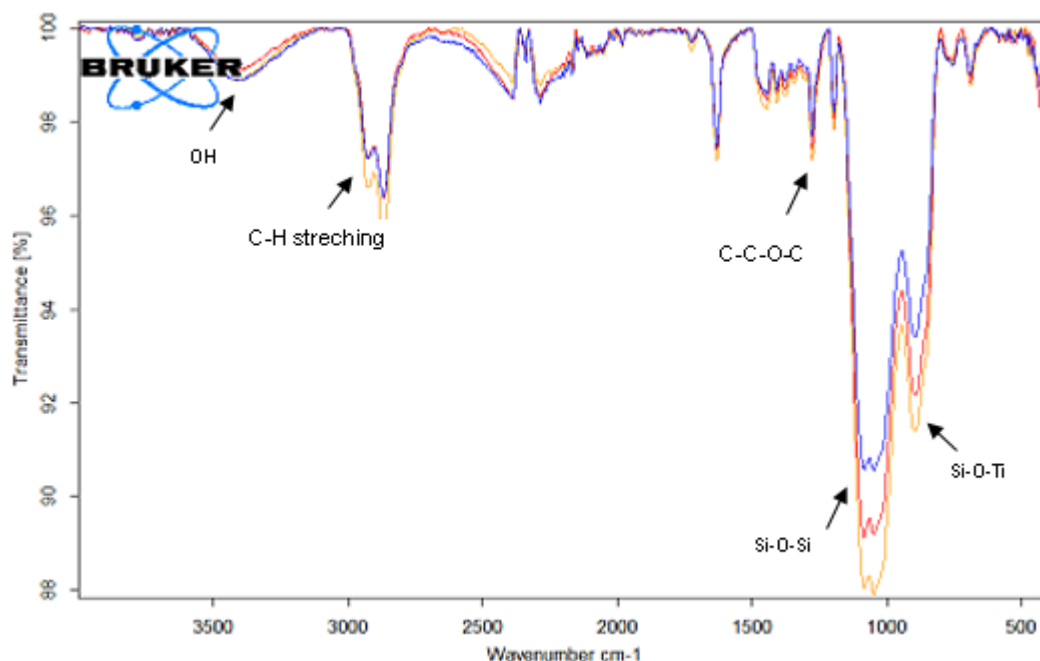
Figure 4. 2 : Comparison of FTIR spectrums of Sample 5, Sampe 14, Sample 23.

The broad band at approximately 3500 cm^{-1} was assigned to O-H stretching of hydroxyl groups. C-H stretching peaks of CH$_2$ links was observed at approximately 2800-2900 cm^{-1} .During the self condensation of epoxy group, ring opens and forms C-C-O-C linear bonds at 1200-1300 cm^{-1} range. When the coating solutions of different prehydrolzing times were compared, it is clearly seen that as the prehyrolysis time increases, the stronger peaks of Si-O-Si, Si-O-Ti and -OH were attained. It was considered that Ti-O-Ti sharp peaks were attained at 400-700 cm^{-1} .As the epoxy group gives self polymerization, ring opens and it is observed that 120 minutes of prehyrolysis time is the best for the cross linking (Si-O-Si) bonds and to get more intense Si-O-Si groups in the system.

4.6 AFM Analyses of the Coating Samples

When the same group of samples were compared by surface morphology and roughness by the AFM analysis, it is clearly seen that the sample 23 has the highest roughness values.

Table 4. 8 : The effect of pre hydrolysis time on roughness**.**

Name	Ti[iOPr]$_4$	H$_2$O	Hydrolysis Time(min)	Roughness (nm)
Sample 5	30 g	10 g	30 min	0,357 nm
Sample 14	30 g	10 g	60 min	0,311 nm
Sample 23	30 g	10 g	120 min	0,660 nm
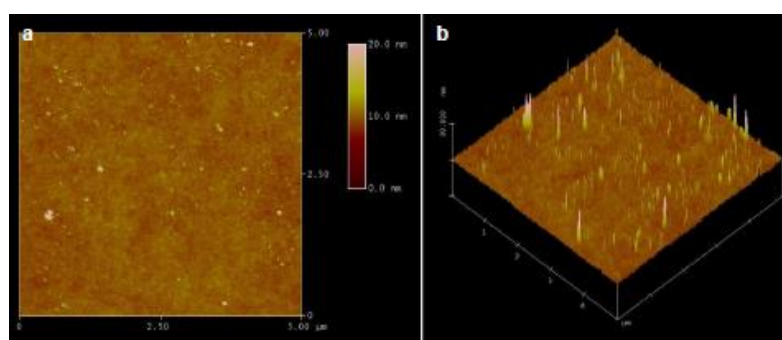
Figure 4. 3 : 5 µm x 5 µm AFM images of Sample 5.
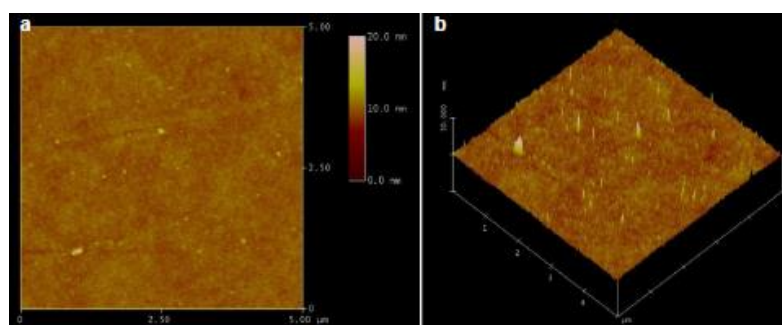
Figure 4. 4 : 5 µm x 5 µm AFM image of Sample 14.
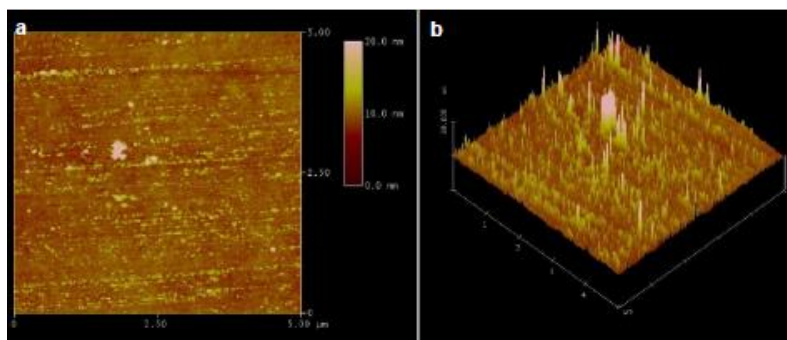
Figure 4. 5 : 5 µm x 5 µm AFM image of Sample 23.

Table 4. 9 : The effect of Titanium(IV) isopropoxide on roughness.

Name	Ti[iOPr]$_4$	H$_2$O	Hydrolysis Time(min)	Roughness (nm)
Sample 20	10 g	10 g	120 min	0,305 nm
Sample 23	30 g	10 g	120 min	0,660 nm
Sample 26	40 g	10 g	120 min	0,304 nm
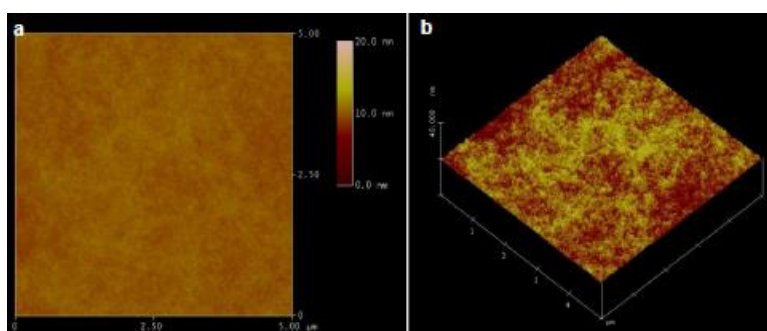
Figure 4. 6 : 5 µm x 5 µm AFM image of Sample 20.
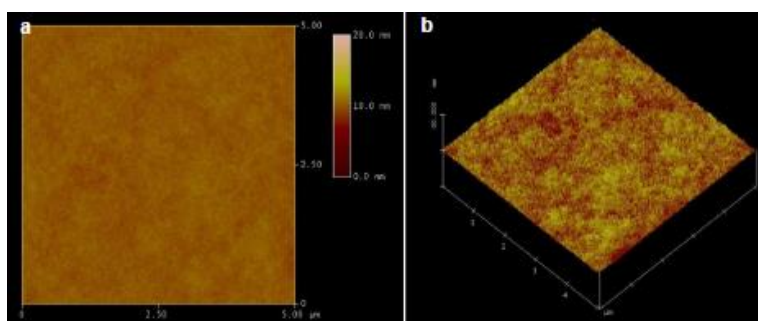
Figure 4. 7 : 5 µm x 5 µm AFM image of Sample 26.

Table 4. 10 : The effect of changing amount of water on roughness.

Name	Ti[iOPr]$_4$	H$_2$O	Hydrolysis Time(min)	Roughness (nm)
Sample 22	30 g	5 g	120 min	0,725 nm
Sample 23	30 g	10 g	120 min	0,660 nm
Sample 24	30 g	20 g	120 min	0,395 nm
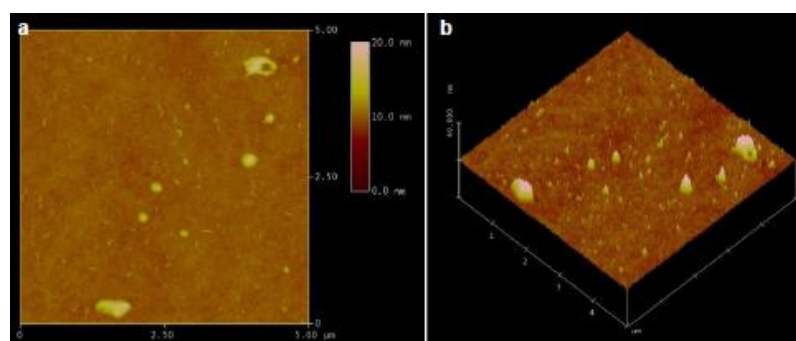
Figure 4. 8 : 5 µm x 5 µm AFM image of Sample 24.
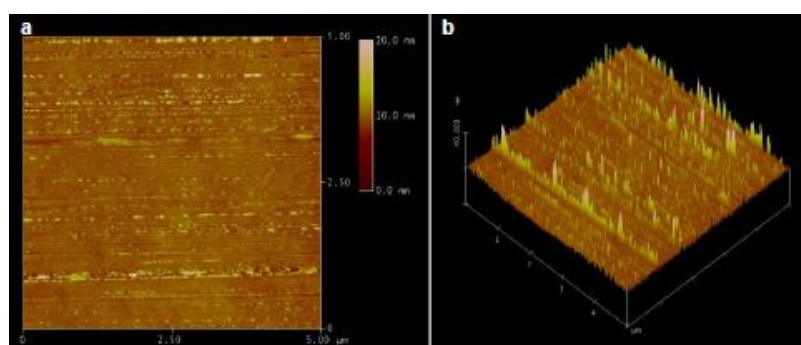
Figure 4. 9 : 5 µm x 5 µm AFM image of Sample 22.

4.7 Optical Spectrum of Measurement

The optical spectroscopy (Figure 4.10) of uncoated and coated sample is compared and it is found that the coating is as transparent as the uncoated glass (Table 5.11).

Table 4. 11 : Optical spectrum of reference sample (Sample 23).

Sample	T_{vis}	T_{sol}	L*	a*	b*
Uncoated	89,8	84	95,9	-96	0,07
Coated	89,8	83,9	95,9	-1,2	0,27
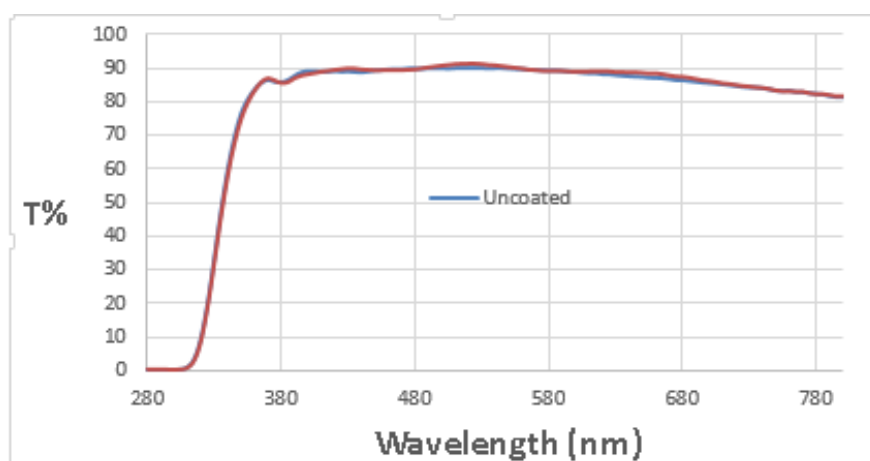
Figure 4. 10 : Transmission – Wavelength graph of reference sample.

4.8 Scratch hardness test

In order to measure scratch hardness, it was performed progressive load in the 5mN and 100 mN range. It was observed that friction force peaks started at 35 mN. All the samples were measured at 50mN constant load and 10 mm/min constant speed. D90 05 sphereoconical tip was used.

Table 4. 12 : Comparison of scratch hardnesses for Sample 5, Sample 14 and Sample 23.

SAMPLE 5 Hardness (Gpa)	SAMPLE 14 Hardness (Gpa)	SAMPLE 23 Hardness (Gpa)
254,18	217,18	247,35
253,56	191,24	305,26
237,55	262,84	273,19
202,85	222,71	225,81
197,3	209,09	254,34
202,57	237,17	253,84
185,71	222,18	245,44
165,87	215,76	190,97
196,72	175,05	202,09
208,87	238,11	252,61
209,22	180,29	202,43
222,56	185,61	168,72
Average: 211,4 GPa	Average: 213,1 GPa	Average: 235,17 GPa

.
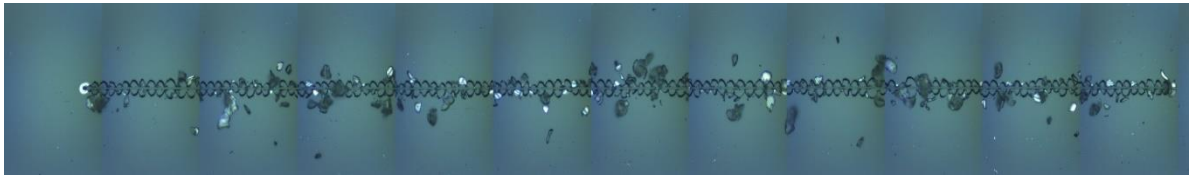
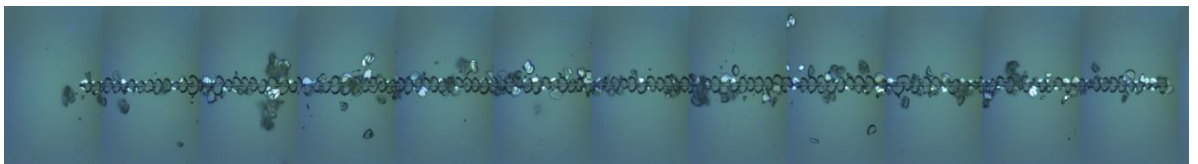**Figure 4. 11 :** Scratch image of Sample 5.


Figure 4. 12 : Scratch image of Sample 14.

Figure 4. 13 : Scratch image of Sample 23.

Table 4. 13 : Titanium (IV) isopropoxide effect on scratch values**.**

Sample	Ti[iOPr]$_4$ /g	H$_2$O / g	Hydrolysis Time (min)	Scratch Hardness (Gpa)
2	10 g	10 g	30 min.	189
5	30 g	10 g	30 min.	211
8	40 g	10 g	30 min.	134
11	10 g	10 g	60 min.	183
14	30 g	10 g	60 min.	213
17	40 g	10 g	60 min.	191
20	10 g	10 g	120 min.	162
23	30 g	10 g	120 min.	235
26	40 g	10 g	120 min.	178

When the samples were compared, the highest scratch values were observed at 30 gr Titanium(IV) isopropoxide. There was no significant change above and below this optimum amount. Consequently, the most scratch resistant coating was Sample 23 among these samples.

4.9 UV-Vis spectrum measurement
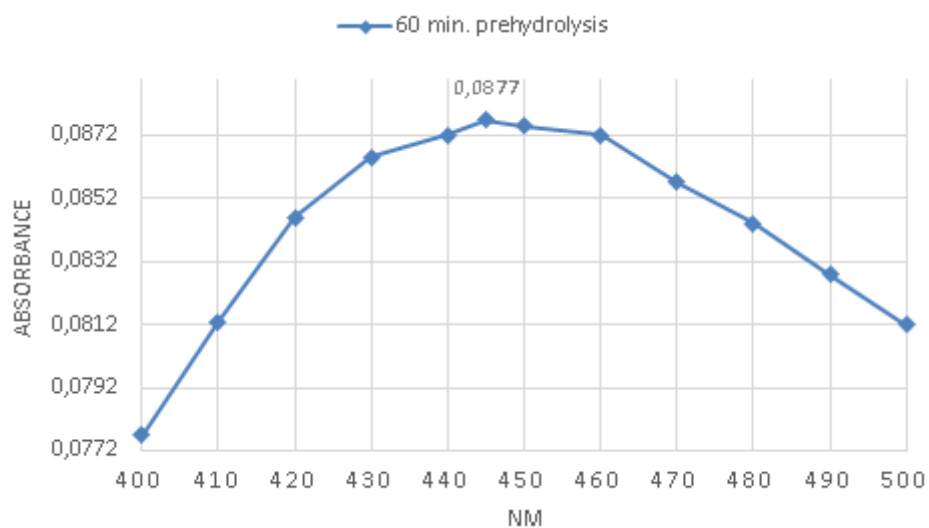
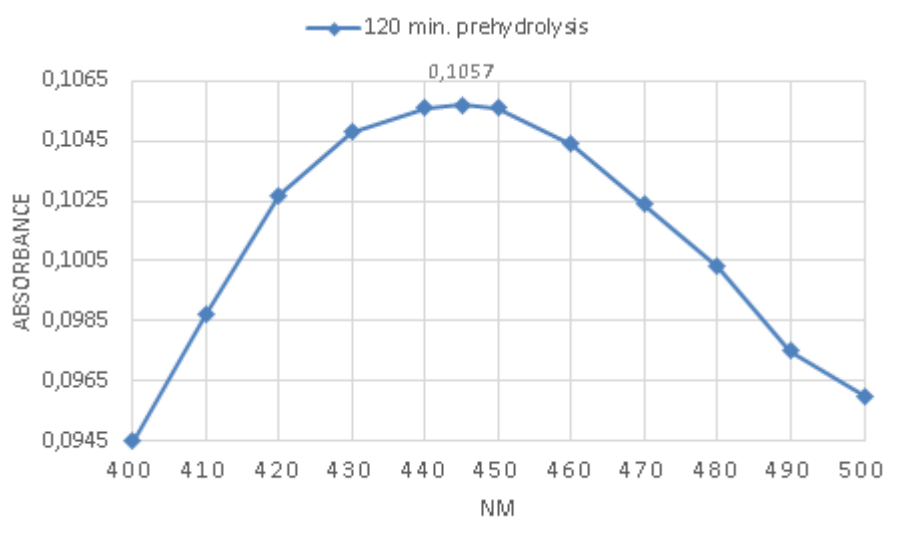**Figure 4. 14 :** Ag absorbance graph at the end of 60 min. pre hydrolysis time.

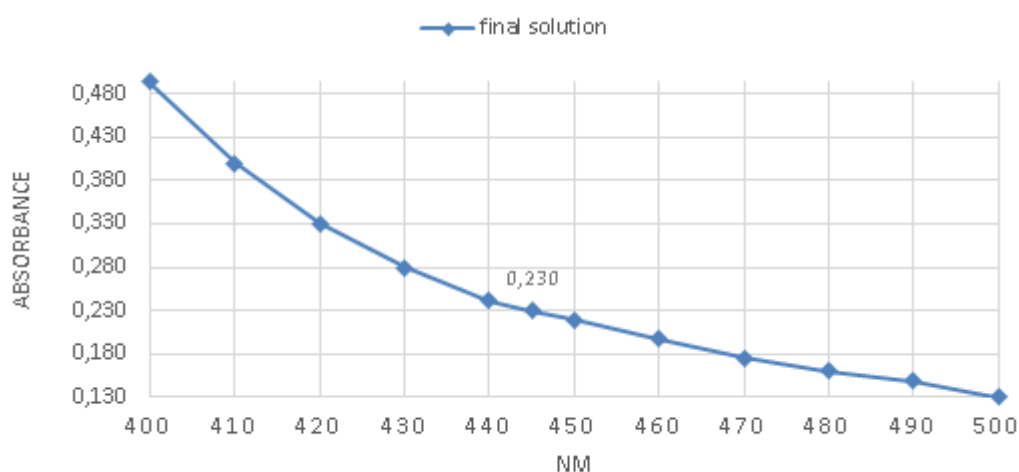**Figure 4. 15 :** Ag absorbance graph at the end of 120 min. pre hydrolysis time.

Figure 4. 16 : Ag absorbance for final solution.

According to the graphics, Ag absorbance increases with time. It means, Ag cations (Ag^+) which have been given to reaction in ethanol turn into Ag (Ag^o) nanoparticles.

4.10 Development of Easy to Clean Property

In order to obtain easy to clean coating, two different compositions were prepared. For the first composition, 1 gr Fluorosilane was added at the end of the coating solution.
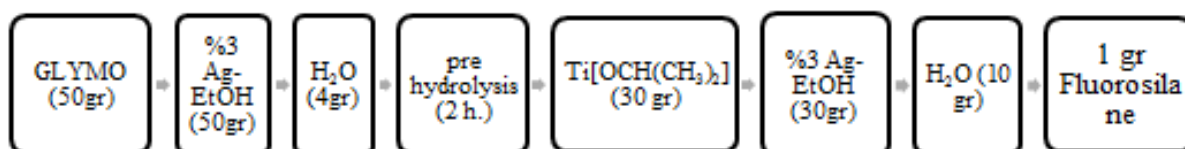
Figure 4. 17 : First composition of easy to clean solution.

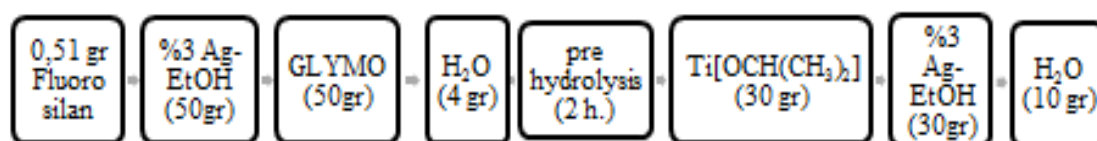For the second composition, 0,51 gr Fluorosilane was mixed with %3 Ag-EtOH and added into GLYMO.

Figure 4. 18 : Second composition of easy to clean solution.

After preparation of solution, glasses were coated at 15cm/min speed by dip coating process and dried in oven at 150°C 30 min.

4.11 Optimization of Easy to Clean Solution

Table 4. 14 : Comparison of physical measurements for two different easy to clean coatings.

Sample Name	%T before abrasion (with apparatus)	%T after abrasion (with apparatus)	Contact angle before abrasion	Contact angle after abrasion	Δ%T
1. composition	36,4	36,2	108	101	-0,2
2. composition	35,2	35	98	99	0,2

It is seen that, the easy to clean coating which the fluorosilane addition is the last stage (first composition) has low scratch resistance than the fluorosilane addition in the first stage (second composition). This shows that the there is a need for fluorosilane to cross link to the network of the coating.

4.12 Comparison of wettability properties

Table 4. 15 : Comparison of wettability properties of final samples**.**

Sample	Contact Angle	Surface Energy (mN/m)
Bare Glass	-	-
Sample 23	62	44,71
1. Hydrophobic composition	108	23,81
2. Hydrophobic composition	98	39,99

In order to calculate surface energy, we used water, diiodomethane, formamide and ethylene glycol liquids. Surface energy was calculated with Fowkes method by contact angle measurement instrument. For uncoated bare glass, contact angle and surface energy could not be measured since the water droplet complately spread on the glass surface. It'seen that there is an inverse proportion between contact angle and surface energy.

4.13 Viscosity Measurements

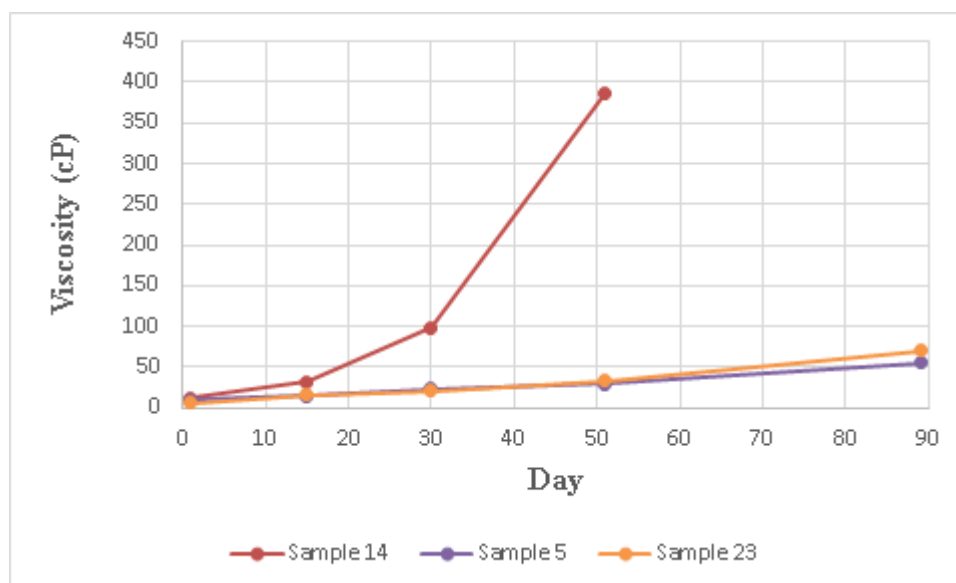Viscosity of the samples were measured periodically at 10 rpm for 3 months.

Figure 4. 19 : Viscosity values of Sample 5, Sample 14 and Sample 23.

It's clearly seen that sample 14 has the highest viscosity and the less shelf life.

4.14 Antibacterial activity of samples

After 12 hours incubation, there is no reproduction on the surface where contact with solid medium. As a result, Sample 23 (referance sample) and 2 different easy to clean compositions were tested by using E.Coli ATCC 11775 and S.Aureus ATCC 25923. It was observed that all 3 samples have log5 (99,999%) reduction.

REFERENCES

[1,20] **Pierre, A.C.,** (1998). Introduction to Sol-Gel Processing, *Kluwer Academic Publishers*, 11 – 89.

[2] **Othmer, K.,** (1994). Encyclopedia Of Chemical Technology, *Wiley Interscience*, *22*, 503.

[3] **Hamilton, D.L.**, **Mackenzie, W.S.**, (1960).
(2000). An Experimental Evaluation of Theory-Based Mother and Mother-Child Programs for Children of Divorce, *Journal of Consulting and Clinical Psychology*, *68*(5), 843 – 856.

[4] **Luth, W.C., Ingamells, C U.,** (1965). Gel preparation of starting materials for hydrothermal experimentation, *American Mineralogist,* 50, 255.

[5] **Hamilton, D.L., Handerson, C.M.B.,** (1968). The Preparation of Silicate Compositions by a Gelling Method, *Mineralogical Magazine*, 36(285), 832-838.

[6] **Biggar, G.M., O'Hara, M.J.,** (1981). A Comparison of Gel and Glass Starting
Materials for Phase Equilibrium Studies, *Mineralogical Magazine*, 37(286), 198-205.

[7] **Dislich, H., Hinz, P.J.,** (1982). *Journal of Non-Crystalline Solids,* 48, 11-16.

[8] **Geffken, W.**, **Berger, E.,** (1943). Anti-reflective Coating, *German Patent 736411,* Jenaer Glasswerk Schott.

[9] **Brinker, C.J., Scherer, G.W.,** (1985). Sol-gel Glass I: Gelation and Gel Structure, *Journal of Non-Crystalline Solids,* 70(3), 301-322.

[10] **Mujahid, A., Lieberzeit, P., Dickert, F.L.,** (2010). Chemical Sensors Based on Molecularity Imprinted Sol-Gel Materials, *Materials,* 3(4), 2196-2217.

[11] **Pohl, E.R., Osterholtz, F.R.,** (1985). Molecular Characterization of Composite Interfaces (eds H. Ishida and G. Kumar), *Plenum Publishing Corporation*, New York, 157.

[12] **Kessle, V.G., Spijksma, G.I., Seisenbaeva, G.A., Hakansson, S., Blank, D.H.A., Bouwmeester, H.J.M.,** (2006). New Insight the Role of Modifying Ligands in the Sol-Gel Processing of Metal Alkoxide Precursors: A Possibility to Approach New Classes of Materials, *Journal of Sol-Gel Science and Technology,* 40(2), 169-179.

[13] **Aurobind, S.V., Amirthalingam, K.P., Gomathi, H.,** (2006). Sol-Gel Based Surface Modification of Electrodes for Electro Analysis, *Advances in Colloidal and Interface Science,* 121, 1-7.

[14] **Maruszewski, K., Strek, W., Jasiorski, M.,** (2003). Technology and Applications of Sol-Gel Materials, *Radiaton Effects & Defects in Solids,* 158, 439-450.

[15] **Iler, R.K.,** (1979). The Chemistry of Silica, *Wiley Interscience*, New York.

[16] **Assink, R.A., Kay, B.D.,** (1988). Sol-Gel Kinetics I: Functional Group Kinetics, *Journal of Non-Crystalline Solids,* 99, 359-370.

[17] **Brinker, C.D., Keefer, K.D., Schaefer, D.W., Assink, R.A., Kay, B.D., Ashley, C.S.,** (1982). Sol-Gel Transition in Simple Silicates II, *Journal of Non-Crystalline Solids,* 63(1), 45-59.

[18] **Tian, B., Zhang, L., Gou, J., Pan, Z., Zhang, Y., Tang, X.,** (2014). A Comparison of the Effect of Temperature and Moisture on the Solid Dispersions: Aging and Crystallization, 475, 385-398.

[19] **Mitrano, D.M., Motellier, S., Clavaguera, S., Nowack, B.,** (2015). Review of Nanomaterial Aging and Transformations Through the Life cycle of Nano-Enhanced Products, *Environment International,* 77, 132-147.

[21] **Niederberger, M., Pinna N.,** (2009). Metal Oxide Nanoparticles in Organic Solvents, *Springer Dordrecht Heidelberg London,* New York, 7-16.

[22] **Livage, J., Henry, M., Sanchez, C.,** (1988). Sol-Gel Chemistry of Metal Oxides, *Solid State Chemistry,* 18, 259-342.

[23] **Rao, A.V., Pajonk, G.M., Parvathy, N.N.,** (1994). Effect of Solvents and Catalysts on Monolithicity and Physical Properties of Silica Aerogels, *Journal of Materials Science,* 29(7), 1807-1817.

[24] **Khaskin, I.G.,** (1952). Several Applications of Deuterium and Heavy Oxygen in the Chemistry of Flint, *Dokl. Akad. Nauk SSSR,* 85, 129.

[25] **Rahaman, M.N.,** (2007). Ceramic Processing, *Taylor & Francis Group CRC Press.*

[26] **Aegerter, M.A., Mennig, M.,** (2004), Sol-Gel Technologies for Glass Producers and Users, *Kluwer Academic Publishers,* New York.

[27] **Brinker, C.J., Hurd, A.J., Frye, G.C., Schunk, P.R., Ashley, C.S.,** (1991). Sol-Gel Thin Film Formation, *Joural of the Ceramic Society of Japan,* 99, 862-877.

[28] **Mennig, M., Schmidt H.,** (2000). Wet Coating Technologies for Glass Sheet Courses, *3rd International Conference on Coatings on Glass.*

[29] **Puetz, J., Aegerter, M.A.,** (2004). Dip Coating Technique, Sol-Gel Technologies for Glass Producers and Users, *Kluwer Academic Publishers,* New York.

[30] **Brinker, C.J., Scherer, G.W.,** (1990). Sol-Gel Science: The Physics and Chemistry of Sol-Gel Processing, *Acedemic Press,* San Diego, USA.

[31] **Katelnikovas, A., Barkauskas, J., Inavauskas, F., Beganskiene, A., Kareiva, A.,** (2007). Aquous Sol-Gel Synthesis Route for the Preparation of YAG: Evaluation of Sol-Gel Process by Mathematical Reggression Model, *Journal of Sol-Gel Science and Technology,* 41, 193-201.

[32] **Mohammadi, M.R., Fray, D.J.,** (2011). Sol-Gel Derived Nanocrystalline and Mesoporous Barium Strontium Titanate Prepared at Room Tempareture, *Particuology,* 9, 235-242.

[33] **Woignier, T., Phalippou, J.,** (2016). Glasses: Sol-Gel Methods, *Reference Module in Materials Science and Material Engineering.*

[34] **Otterstein, E., Karapetyan, G., Nicula, R., Stir, M., Schick, C., Burke, E.,** (2008). Sol-Gel Synthesis and Characterisation of Fine-Grained Ceramics in the Alumina-Titania System, *Thermochimica Acta,* 486(1-2), 10-14.

[35] **Owens, G.J., Singh, R.K., Foroutan, F., Alqaysi, M., Han, C.M., Mahapatra, C., Kim, H.W., Knowles, J.C.,** (2016). Sol-Gel Based Materials for Biomedical Applications, *Progress in Materials Science,* 77, 1-79

[36] **Fan, H., Cheng, Y., Gu. C., Zhou, K.,** (2016). A Novel Gas Sensor of Formaldehyde and Ammonia Based on Cross Sensitivity of Cataluminescence on Nano Ti3SnLa2O11, *Sensors and Actuators B Chemicals,* 223, 921-926.

[37] **Liu, B., Lin, X., Zhu, L., Wang, X., Xu, D.,** (2014). Fabrication of Calcium Zirconate, Fibers by the Sol-Gel Method, *Ceramics International,* 40(8), 12525-12531.

[38] **Guizard, C.,** (1996). Chapter 7 : Sol-Gel Chemistry and Its Application to Porous Membrane Processing, *Membrane Science and Technology*, 4, 227-258.

[39] **Rezaei V., Restegarzadeh, S.,** (2015). Sol-Gel Based Optical Sensor For Determination of Fe(II): A Novel for Iron Speciation, *Spectrohimica Acta,* 136, 832-837.

[40] **Chen, W., Shen, H., Zhu, X., Xing, Z., Zhang, S.,** (2015). Effect of Citric Acid on Structure Photochromic Properties of WO3-TiO2-ZnO Composite Films Prepared by Sol-Gel Method, *Ceramics International,* 41(10), 12638- 12643.

[41] **Ian, Y.Y.,** (2016). Sol-Gel Production of ZnO:CO; Effect of Post Annealing Temperature on Its Optoelectronic Properties, *Materials Science in Semiconductor Processing,* 41, 240-245.

[42] **Guo D., Gong, Y., Wang, C., Shen, Q., Zhang, L.,** (2013). Dielectric and Ferroelectric Properties of $BaTi_2O_5$ Thin Films Prepared by Sol-Gel Method, *Materials Letters,* 95, 55-58.

[43] **Periyat, P., Ullattil, S.G.,** (2015). Sol-Gel Derived Crystalline ZnO Photoanode Film for Dye Sensitized Solar Cells, *Materials Science in Semiconductor Processing,* 31, 139-146.

[44] **Kiraz, N., Burunkaya, E., Kesmez Ö., Asiltürk, M., Çamurlu, H.E., Arpaç, E.,** (2010). Sol-Gel Synthesis of 3-(Triethoxysilyl)propylsuccinicanhydrade Containing Flourinated for Hydrophobic Surface Applications, *Journal of Sol-Gel Science and Technology,* 56, 157-166.

[45] **Pal, S., Tak, Y.K., Song, J.M.,** (2007). Does the Antibacterial Activity of Silver Nanoparticles Depend on the Shape of the Nanoparticle? A Study of Gram-negative Bacterium Escherichia Coli, *Application of Environmental Microbiology,* 73(6), 1712-1720.

[46] **Allafchian, A.R., Bahraman, H., Jalali, S.A.H., Ahmandvand, H.,** (2015). Synthesis, Characterisation and Antibacterial Effect of New Magnetically Core-Shell Nanocomposites, *Journal of Magnetism and Magnetic Materials,* 349, 318-324.

[47] **Campoccia, D.,** (2013). A Review of the Biomaterials Technologies for Infection –resistant Surfaces, *Biomaterials,* 34, 8533-8554.

[48] **Palmer, J., Flint, S., Brooks, J.,** (2007). Bacterial Cell Attachment , The Beginning of A Biofilm, *Journal of Industrial Microbiology & Biotechnology,* 34, 577-588.

[49] **Verran, J., Whitehead, K.,** (2005). Factors Effecting Microbial Adhesion to Stainless Steel and Other Materials Used in Medical Devices, *International Journal of Artificial Organs*, 28, 1138-1145.

[50] **Anselme, K., Davidson, P., Popa, A.M., Giazzon, M., Liley, M., Ploux, L.,** (2010). The Onteraction of Cell and Bacteria With Surfaces

Structured at the Nanometer Scale, *Acta Biomaterials,* 10, 3824-3846.

[51] **Jalali, S.A.H., Allafchian, A.R.,** (2016). Assessment Of Antibacterial Properties Of Novel Silver Nanocomposite, *Journal of the Taiwan Institute of Chemical Engineers,* 59, 506-513.

[52] **Awasthi, K.K., Awasthi, A., Kumar, N., Ray, P., John, P.J.,** (2013). Silver Nanoparticle Induced Cytotoxicity , Oxidative Stress and DNA Damage in CHO Cell, *Journal of Nanoparticle Research,* 15, 1898.

[53] **Liau, S.Y., Read, D.C., Pugh, W.J., Furr, J.R., Russel, A.D.,** (1997). Interaction of Silver Nitrate with Identifiable Groups-Relationship to the Antibacterial Action of Silver Ions, *Letters in Applied Microbiology,* 25, 273-283.

[54] **Yuan, Y., Lee, T.R.,** (2013). Contact Angle and Wetting Property, *Springer Series in Surface Science Techniques,* 51, 3-34.

[55] **Koopal, L.K.,** (2012). Wetting Of Solid Surfaces: Fundamental And Charge Effects, *Advances In Colloidal And Interface Science,* 179-182, 29-42.

[56] **Goldstein, I.J., Newbury, D.E., Echlin, P., Joy, D.C., Romig, A.D., Lyman, C.E., Fiori C., Lifshin, E.,** (1992). Scanning Electron Microscopy And X-Ray Microanalysis, *Plenum Press,* New York, ISBN 0-306-44175-6.

[57] (1999). Energy Dispersive X-Ray Microanalysis – An Introduction, *Wisconsin NORAN Instruments Middleton.* www.noran.com

[58] **Braga, P.C., Ricci , D.,** (2004). Atomic force Microscopy, Biomadical methods and applications, *Humana press incorporation,* 242, 7.

[59] **Ovijid, C., Parekh, S.H., Lam, W., Fletcher, A.,** (2009). Combined Atomic Force Microscopy And Side-View Optical Imaging For Mechanical Studies Of Cell, *Nature Methods,* 6, 383-387.

[60] **Noguchi, T.,** (2001). Detection Of Protein Cofactor Interactions By Means Of Fourier Transform Spectroscopy, *Riken Review, Focused On Bioarchitect Research,* 41, 41- 42.

[61] **Amand, L.E., Tullin, C.J.,** The Theory Behind FTIR Analysis, Presentation At The Swedish National Testing And Research Institute.

[62] **Su, C., Xu, Y., Gong, F., Wang, F., Li, C.,** (2010). The Abrasion Resistance Of A Superhydrophobic Surface Comprised Of Polyurethane Elastomer, *Soft Materials,* 6, 6068-6071.

[63] **Mishra, P.C., Mukherjee, S., Nayak, S.K., Panda, A.,** (2014). A Brief Review Of Viscosity Of Nanofluids, *International Nano Letters,* 4, 109-120.

[64] **Cross, M.M.,** (1965). Rheology Of Non-Newtonian Fluids : A New Flow Equation For Psuedoplastic Systems, *Journal Of Colloid Science,* 20, 417-437.

[65] **Silberberg, A., Eliassaf, J., Katchalsky, A.,** (1957). Temperature Depend Of Light Scattering And Intrinsic Viscosity Of Hydrogen Bonding Polymers, *Journal Of Polymer Science,* 23(103), 259-284

[66] **Günay, V.,** (1990). Sol Gel Processing Of Fibre Reinforced Glass And Glass Ceramics Matrix Composites, *PhD Thesis, University Of Sheffield.*

[67] **Davis, J.T., Rideal, E.K.,** (1963). Interfacial Phenomena, *Academic Press,* New York.

[68] **Wiley, J., Hench, R.R., Ulrich, D.R.,** (1986). Science Of Chemical Ceramic Processing, *John Wiley & Sons,* New York.

[69] **Lev, O., Tsionsky, M., Rabinovich, L.I., Glezer, V., Sampath, S., Pankratov, I., Gun, J.,** (1995). Organically Modified Sol Gel Sensors, *Analytical Chemistry,* 67(1), 22A-30A.

[70] **Landau, L., Levich, B.,** (1942). Dragging Of A Liquid By A Moving Plate, *Acta Physisochem.,* 7, 42-54.

[71] **Wabes, B.D., Oliver W.C.,** (1990). Mechanical Properties Of Sol Gel Coatings, *Journal Of Non-Crystalline Solids,* 121, 348-356.

[72] **Zare, Y.,** (2016). Study Of Nanoparticles Aggregation/Agglomeration In Polymer Particulate Nanocomposites By Mechanical Properties, *Composites Part A: Applied Science And Manufacturing,* 84, 158-164.

[73] **Popall, M., Kappel, J., Pilz, M., Schulz, J., Feyder, G.,** (1994) *Sol Gel Science And Technology,* 2 , 157

[74] **Philliph, G., Schmidt, H.,** (1984). New Materials For Contact Lenses Prepared From Si- And Ti- Alkoxides By The Sol Gel Process, *Journal Of Non-Crystalline Solids,* 63, 283-292.

[75] **Cardiano, P., Sergi, S., Lazzari, M., Piratino, P.,** (2002). Epoxy Silica Polymers As Restoration Polymers, *Polymer Journal,* 43(25), 6635-6640.

[76] **Innocenzi, P., Brusatin, G., Guglielmi, M., Signorini, R., Meneghetti, M., Bozio, R., Maggini, M., Scorrano, G., Prato, M.,** (2000). Optical Limiting Deviced Based On C-60 Derivatives In Sol Gel Hybrid Organic-Inorganic Materials, *Journal Of Sol Gel Science And Technology*,1-3 (19), 263-266.

[77] **Henriette, M.C.,** (2009). Nanocomposites For Food Packaging Applications, *Food Research International*, 42, 1240-1253.

[78] **Callies, M., Quere, D.,** (2005). On Water Repellency, *Soft Matter*, 1(1), 55-61.

[79] **Innocenzi, P., Figus, C., Kidchob, T.,** (2011). Crystallization In Organic-Inorganic Hybrid Materials Through-Self Organization From 3-Glycidoxypropyltrimethoxysilane, *Journal Of The Ceramic Society In Japan,* 119(6), 387-392.

[80] **Dash, S., Mishra, S., Patel, S., Mishra, B.,K.,** (2008). Organically Modified Silica : Synthesis And Applications Due To Its Surface Interaction With Organic Molecules, *Advance Colloidal Interface Science*, 140, 77-94.

[81] **Fujishima, M., Takatori, H., Tada, H.,** (2011). Interfacial Chemical Bonding Effect On The Photocatalytic Activity Of Tio2-Sio02 Nanocoupling Systems, *Journal Of Colloidal Interface Science*, 361, 628-631.

[82] **Kong, D., Du, X., Wei, S., Zhang, H., Yang, Y., Shah, S.,** (2012). Influence Of Nanosilica Agglomeration On Microstructure And Properties Of The Hardened Cement –Based Materials, *Construction And Building Materials,* 37, 707-715

[83] **Jamani Ketek Lahijaniya, Y., Mohsen, M., Bastani, S.,** (2014). Characterization Of Mechanical Behavior Of Uv Cured Urethane Acrylate Nanocomposite Films Loaded With Silane Treated Nanosilica By The Aid Of Nanoindentation And Nanoscratch Expdriments, *Tribology International*, 69, 10-18.

[84] **Schneider, J., Schula, S., Weinhold, W.P.,** (2012). Characterization Of The Scratch Resistance Of Annealed And Tempered Architectural Glass, *8th International Conference On Coatings On Glass And Plastics — ICCG8*, 520(12), 4190-4198.

[85] **Cook, R.F., Roach, D.H.,** (1986). The Effect Of Lateral Crack Growth On The Strength Of Contact Flows In Brittle Materials, *Journal Of Material Research*, 1(4), 589-600.

[86] **Langroudi, A.E.,** (2013). A Brief Review Of Nanoindentation Techniwue And Its Applications In Hybrid Nanocomposite Coatings, *International Journal Of Bio-Inorganic Hybrid Nanomaterials*, 2, 337-344.

[87] **Mullins, W.M., Wereszczak, A., Curzio, E.L.,** (2007). Synthesis And Processing Of Nanostructured Materials: Ceramic Engineering And Science Proceeding, *The American Ceramic Society*, 27 (8), 41-47.

[88] **Hernandez, J.,H.,** (2016). Antimicrobial Micro/Nanostructured Functional Polymer Surfaces: Chapter 5, *Nanobiomaterials In Antimicrobial Therapy*, 6, 153-192.

[89] **Extremina, C.I., Fonseca, A.F., Granja, P.L., Fonseca, A.P.,** (2010). Anti-Adhesion And Antiproliferative Cellulose Triacetate Membrane For Prevention Of Biomaterial-Centred Infections Associated With Staphylococcus Epidermidis, *International Journal Of Antimicrobial Agents*, 35(2), 164-168.

[90] **Owen, T.,** (1996). Fundamentals Of Uv-Vis Spectroscopy, *Hewlett Packard Company*, Germany.

APPENDIX

Appendix A : Distributions of contents for other experiment sets measured by SEM-EDS.
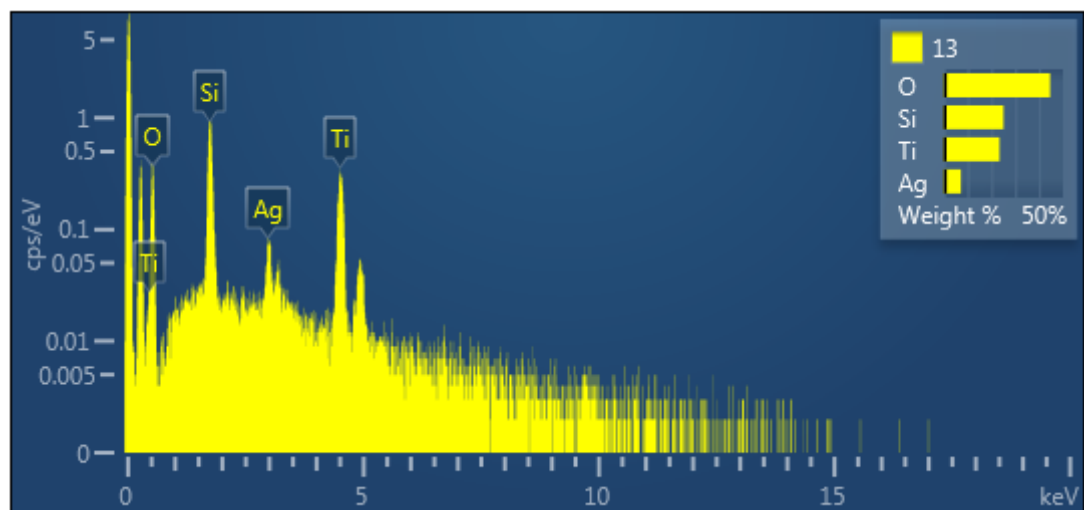
Figure A. 1 : Distributions of contents for sample 13.
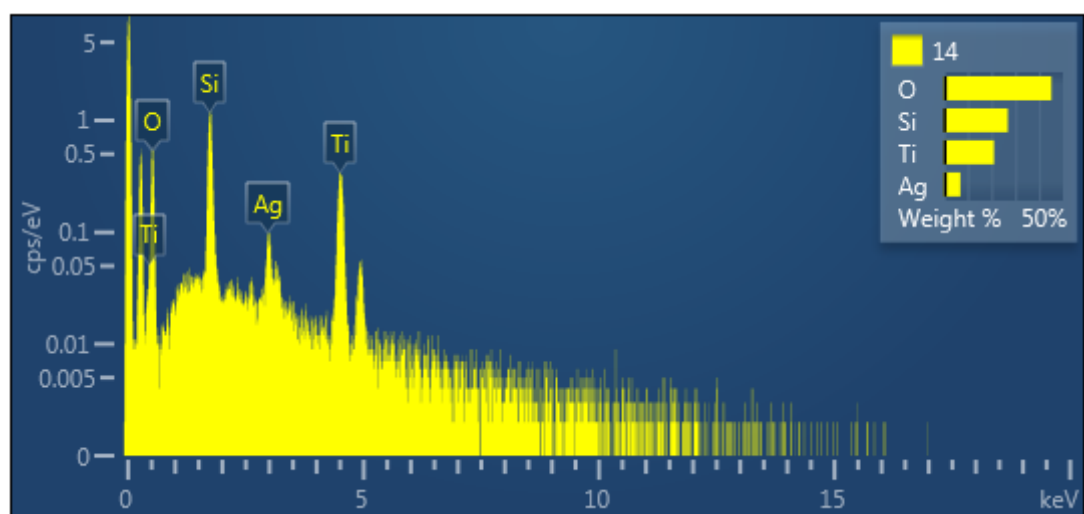
Figure A. 2 : Distributions of contents for sample 14.
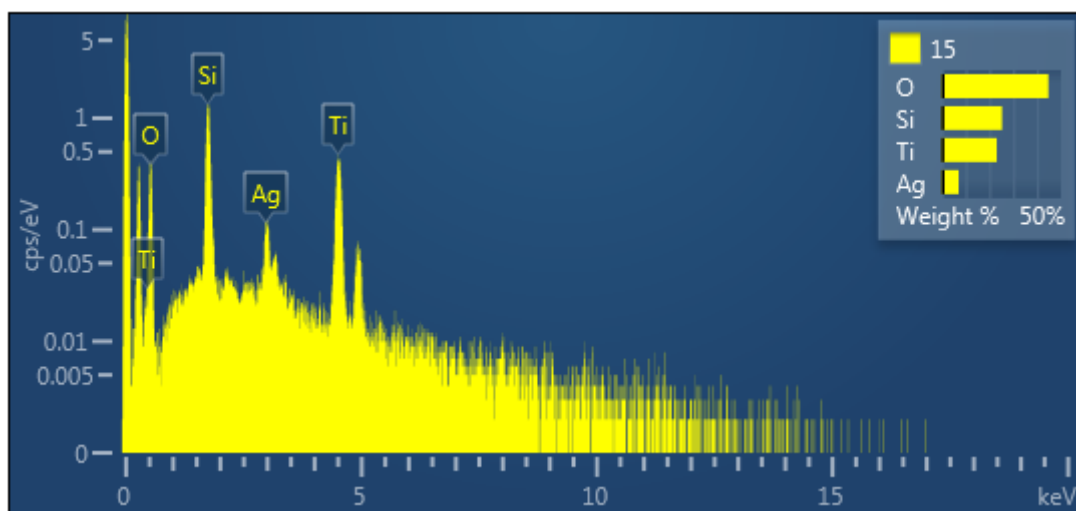
Figure A. 3 : Distributions of contents for sample 15.
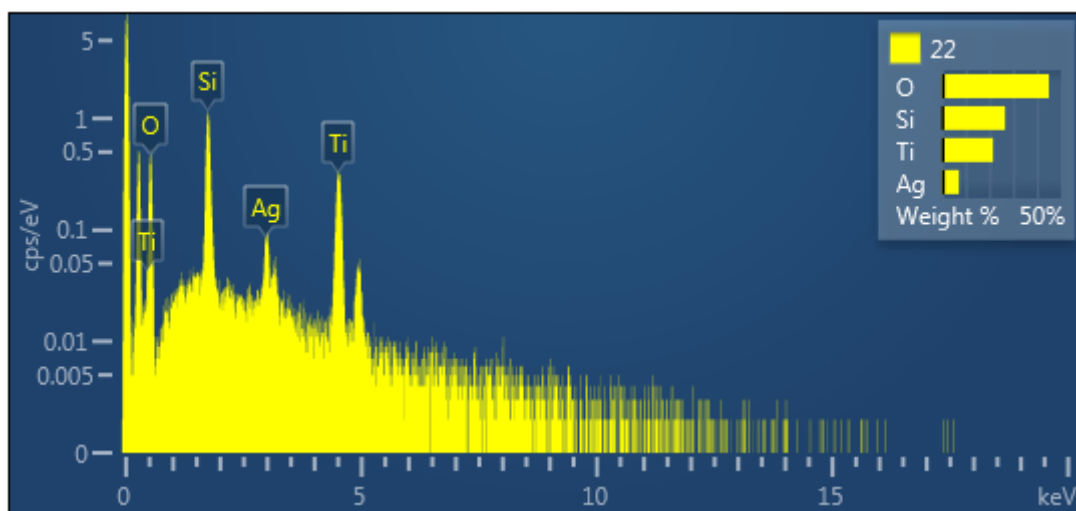
Figure A. 4 : Distributions of contents for sample 22.
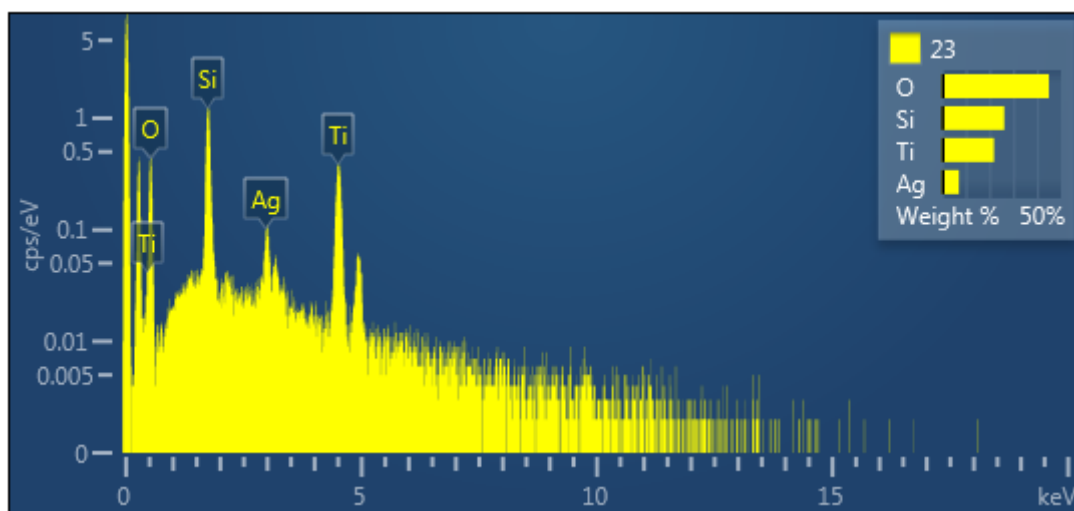
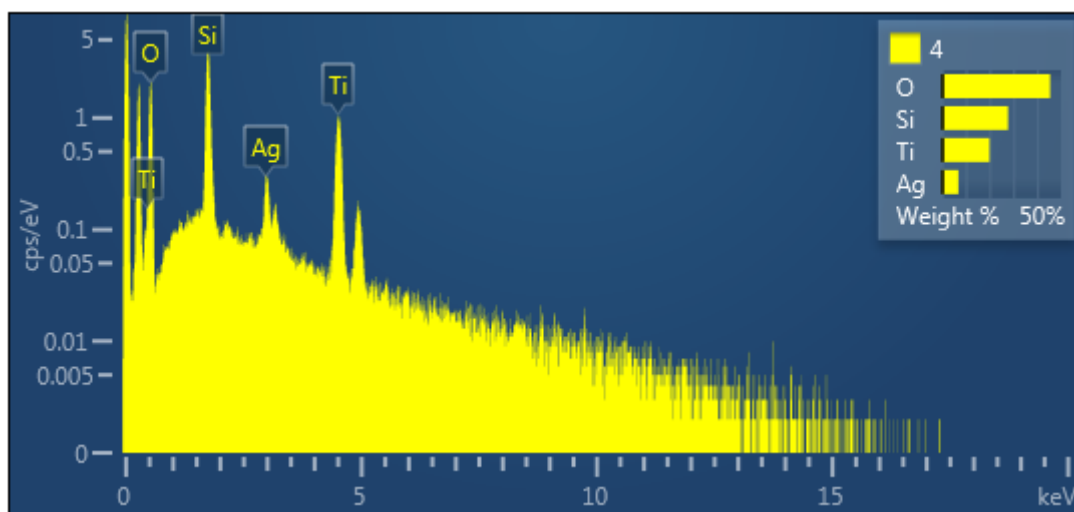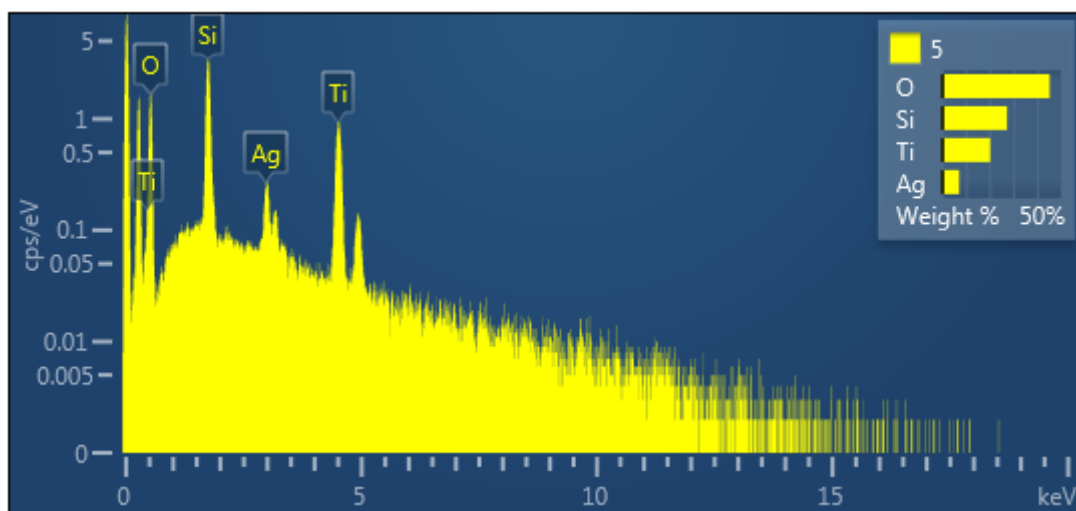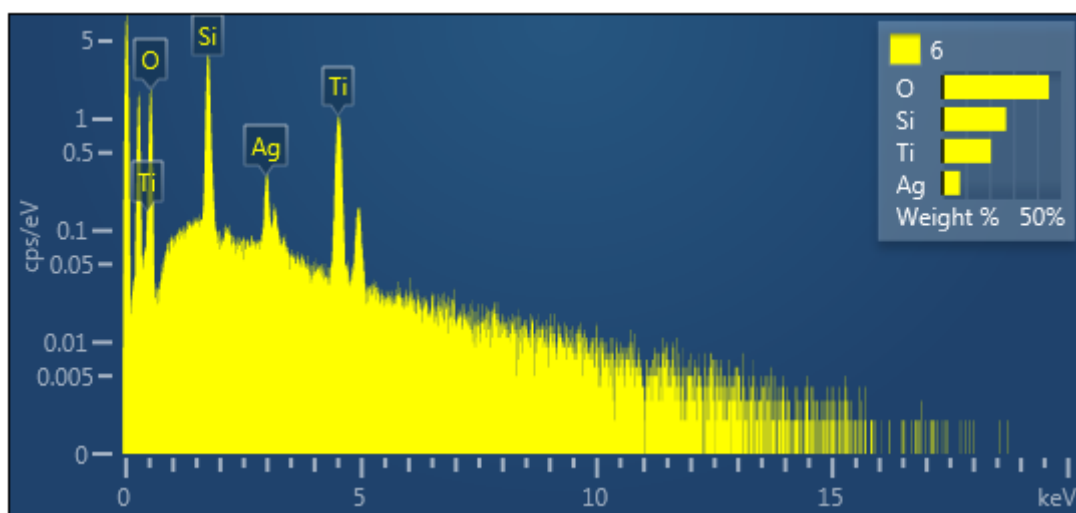**Figure A. 5 :** Distributions of contents for sample 23.
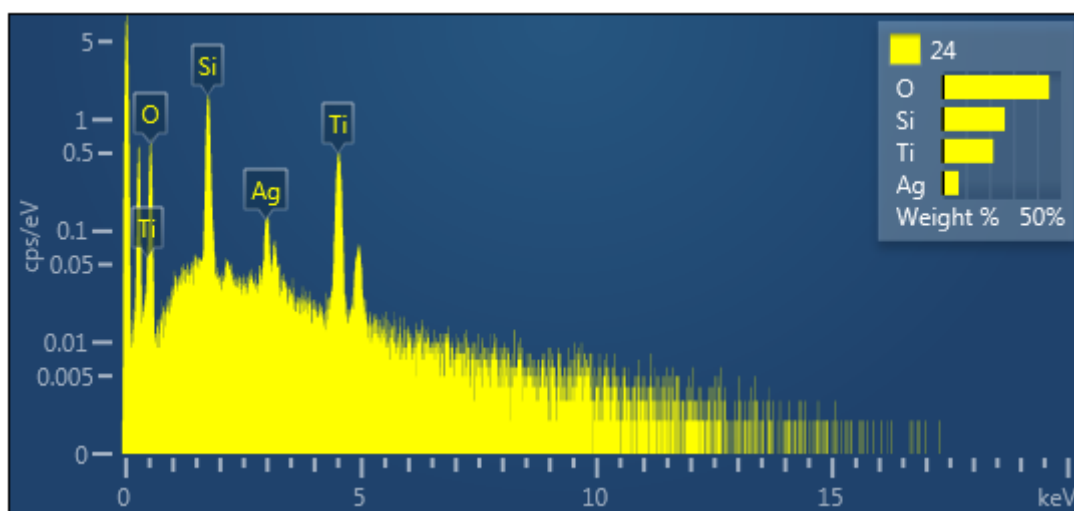
Figure A. 6 : Distributions of contents for sample 24.

Figure A. 7 : Distibutions of contents for sample 4.

Figure A. 8 : Distributions of contents for sample 5.

Figure A. 9 : Distributions of contents for sample 6.
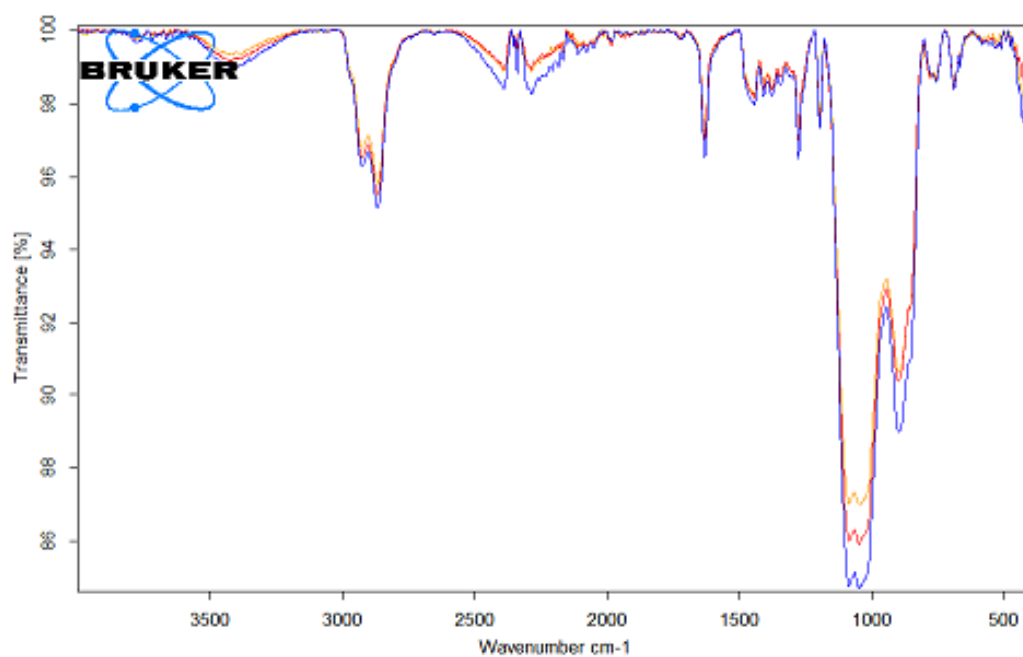
FTIR peaks of other experiment sets.
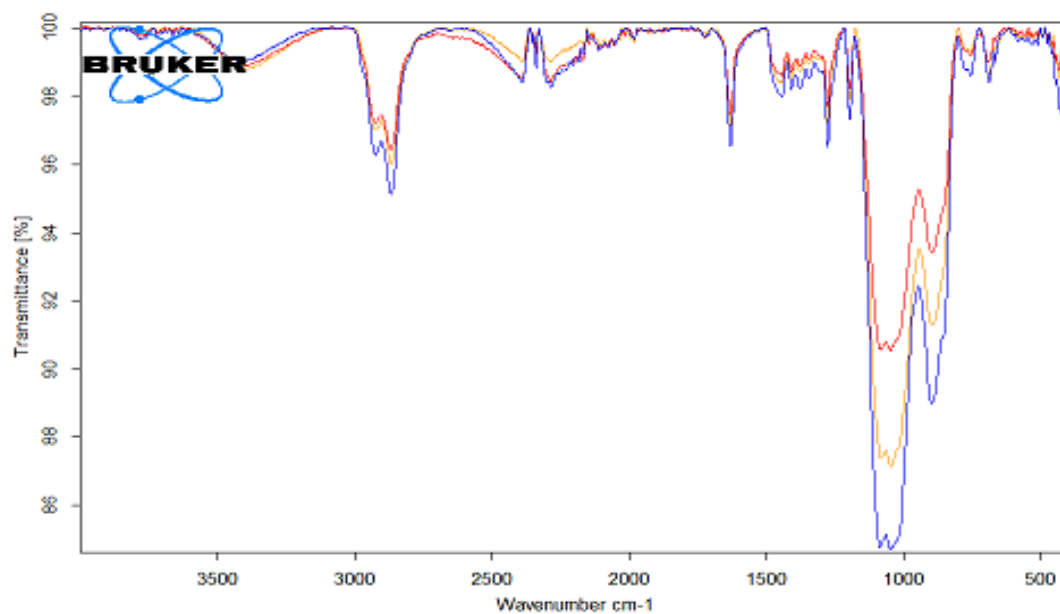
Figure B. 1 : Comparison of FTIR peaks for Sample 4 (blue), Sample 5 (red),
Sample 6 (yellow).
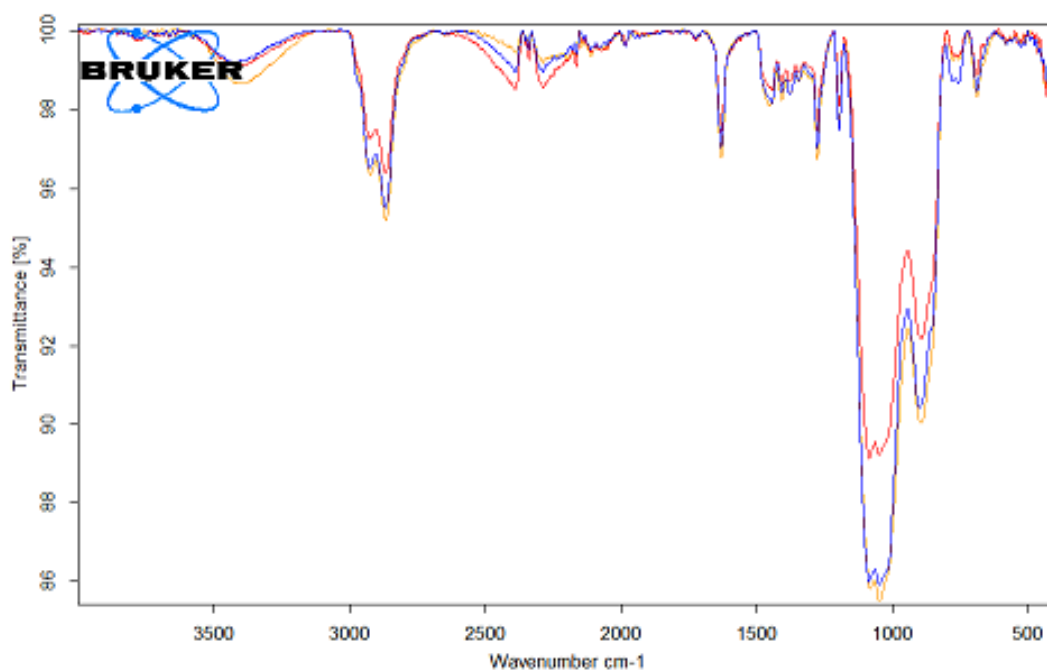
Figure B. 2 : Comparison of FTIR peaks for Sample 13 (blue), Sample 14 (red),
Sample 15 (yellow).
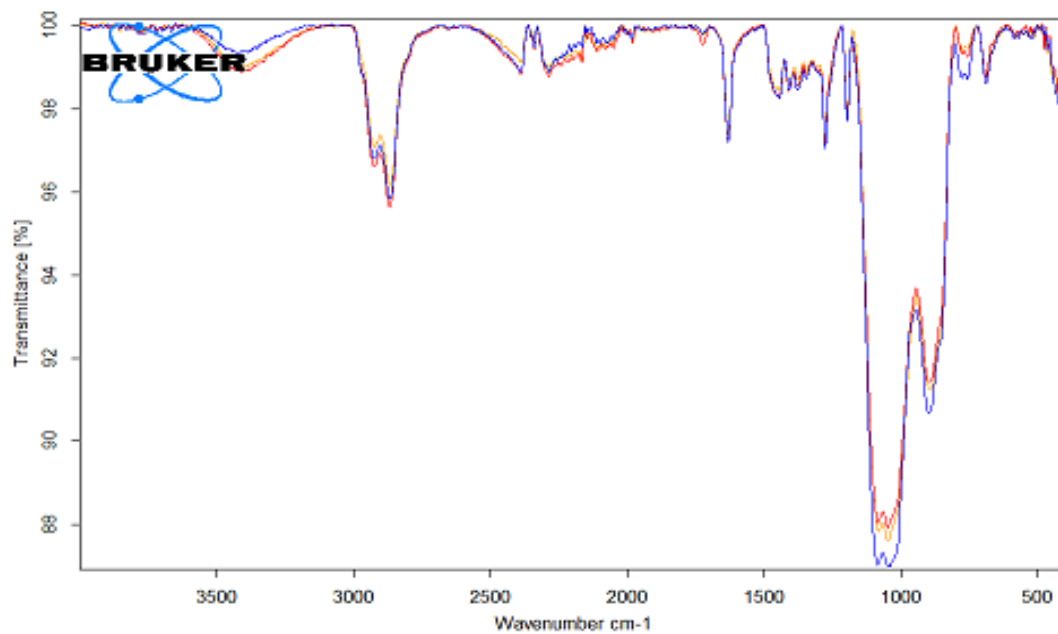
Figure B. 3 : Comparison of FTIR peaks for Sample 22 (blue), Sample 23 (red), Sample 24 (yellow).

Figure B. 4 : Comparison of FTIR peaks for Sample 4 (blue), Sample 13 (red), Sample 22 (yellow).
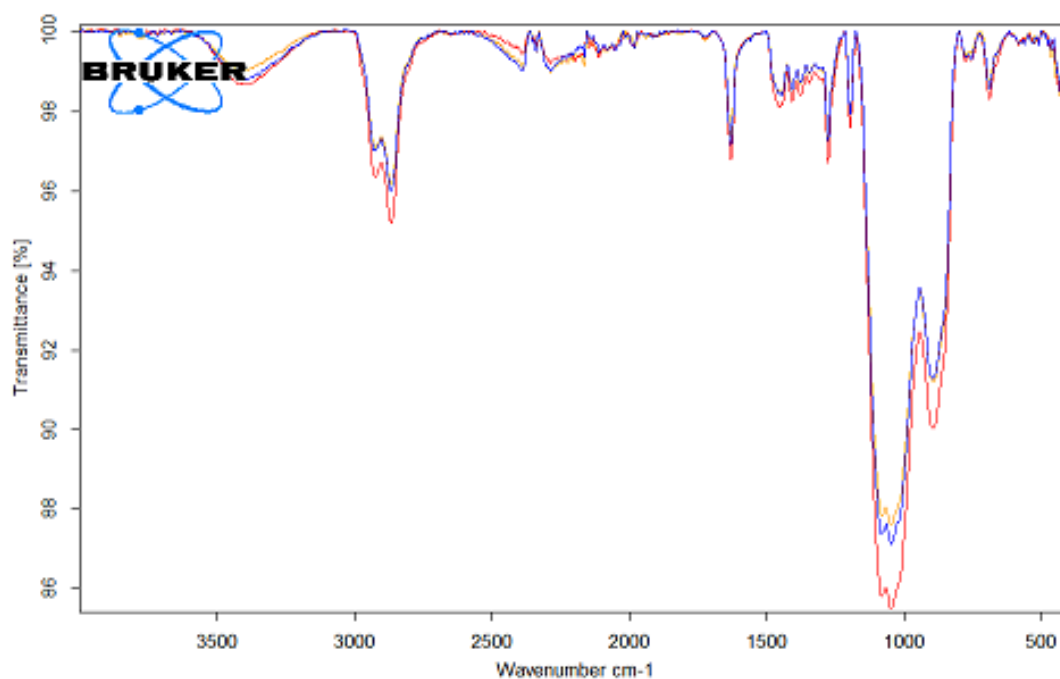
Figure B. 5 : Comparison of FTIR peaks for Sample 6 (blue), Sample 15 (red), Sample 24 (yellow).

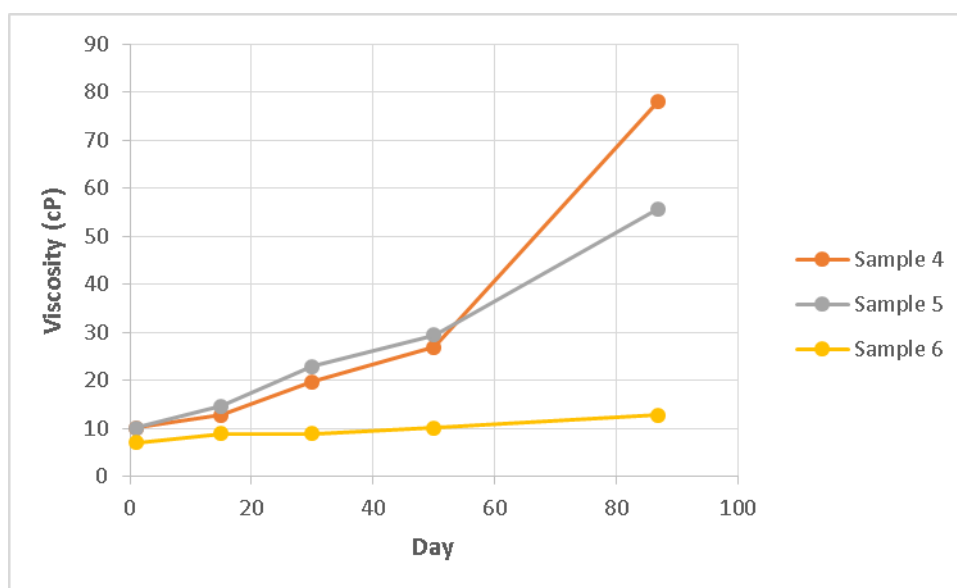**Appendix C :** Viscosity measurements of other experiment sets.

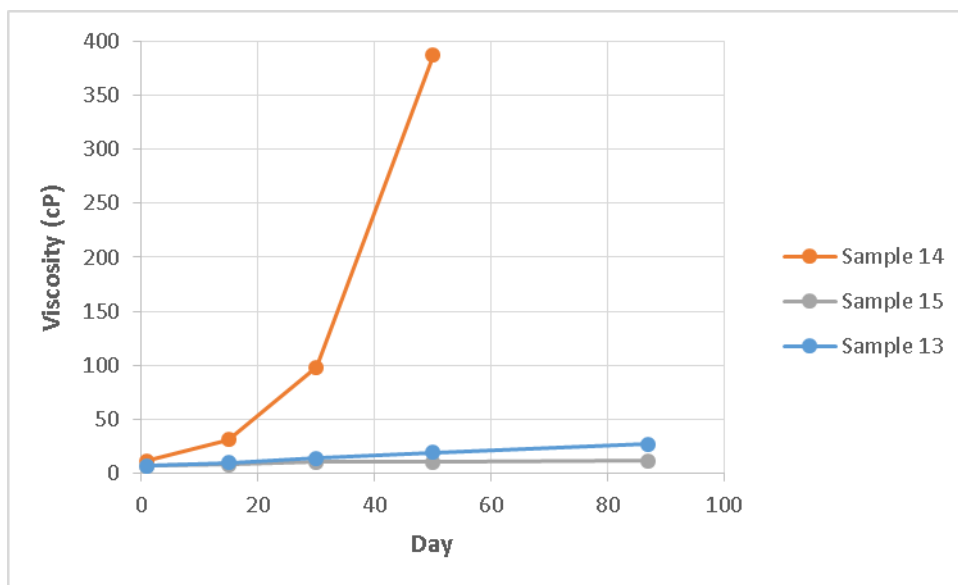**Figure C. 1 :** Comparison of viscosity for Sample 4, Sample 5, Sample 6.

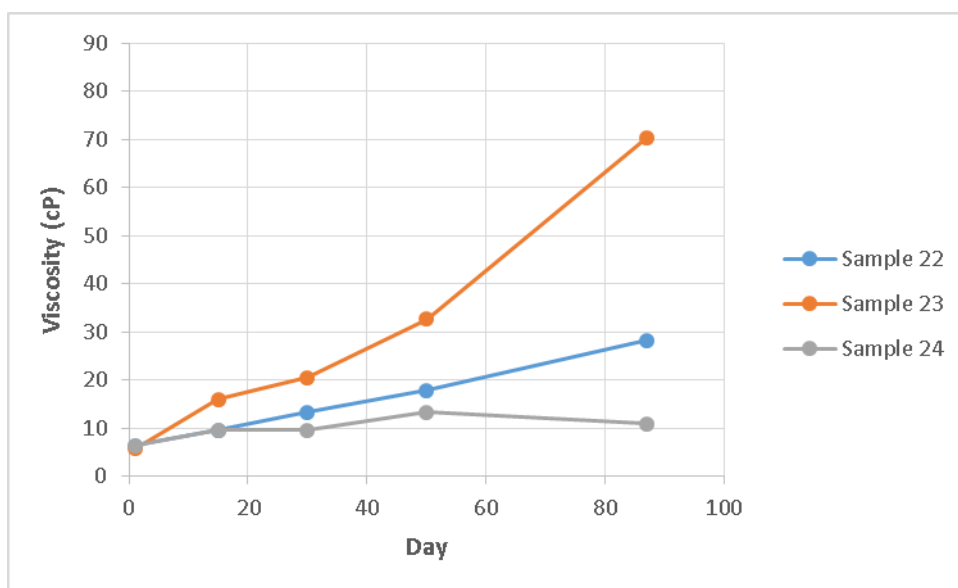**Figure C. 2 :** Comparison of viscosity for Sample 13, Sample 14, Sample 15..

Figure C. 3 : Comparison of viscosity for Sample 22, Sample 23, Sample 24.

CURRICULUM VITAE

Name Surname: Beyza Yedikardeş

Place and Date of Birth: İstanbul/Üsküdar – 09.08.1992

E-Mail: beyzayedikardes@gmail.com

EDUCATION:

- **M. Sc. :** Istanbul Technical University – Nanoscience and Nanoengineering (2014-2016)

- **B. Sc. :** Yıldız Technical University – Chemistry (2010 - 2014)

EXPERIENCES

Project Intern: 08/2015 – 08/2016, Şişecam, Science and Technology Center, Department of Atmospheric Coatings

Project Intern: 02/2013-05/2014, Cerrahpaşa Medical Faculty, Department of Biochemistry

Intern: 06/2013-08/2013, Cerrahpaşa Medical Faculty, Fikret Biyal Research Laboratory